Federated Learning Resilient to Byzantine Attacks and Data Heterogeneity

Shiyuan Zuo, Xingrun Yan, Rongfei Fan, Member, IEEE, Han Hu, Member, IEEE, Hangguan Shan, Senior Member, IEEE, Tony Q. S. Quek, Fellow, IEEE, and Puning Zhao

Abstract—This paper addresses federated learning (FL) in the context of malicious Byzantine attacks and data heterogeneity. We introduce a novel Robust Average Gradient Algorithm (RAGA), which uses the geometric median for aggregation and allows flexible round number for local updates. Unlike most existing resilient approaches, which base their convergence analysis on stronglyconvex loss functions or homogeneously distributed datasets, this work conducts convergence analysis for both strongly-convex and non-convex loss functions over heterogeneous datasets. The theoretical analysis indicates that as long as the fraction of the data from malicious users is less than half, RAGA can achieve convergence at a rate of $\mathcal{O}(1/T^{2/3-\delta})$ for non-convex loss functions, where T is the iteration number and $\delta \in (0, 2/3)$. For strongly-convex loss functions, the convergence rate is linear. Furthermore, the stationary point or global optimal solution is shown to be attainable as data heterogeneity diminishes. Experimental results validate the robustness of RAGA against Byzantine attacks and demonstrate its superior convergence performance compared to baselines under varying intensities of Byzantine attacks on heterogeneous datasets.

Index Terms—Federated learning, Byzantine attack, data heterogeneity, robust aggregation.

I. INTRODUCTION

THE rapid growth of intelligent applications in recent decade promotes a broad adoption of them on various devices or equipments, such as mobile phones, wearable devices, and autonomous vehicles, etc [1]–[3]. To enable one intelligent application, raw data from various subscribed users has to be trained together to generate a uniform model. From the perspective of subscribed users, who may distribute broadly, it has a risk of privacy leakage if they offload their raw data to a central server for training [4], [5]. Federated learning (FL) is a distributed training framework and has emerged

Manuscript received December 17, 2024; revised April 17, 2025; accepted May 14, 2025. This paper is supported by Joint Funds of the National Natural Science Foundation of China (NSFC) No. U2336211, NSFC under Grant No. 62171034, No. 92467206, and is also supported by National Key Research and Development Program of China. (Corresponding Author: Rongfei Fan).

S. Zuo, X. Yan, and R. Fan are with the School of Cyberspace Science and Technology, Beijing Institute of Technology, Beijing 100081, China (e-mail: {zuoshiyuan, 3220221473, fanrongfei}@bit.edu.cn); H. Hu is with the School of Information and Electronics, Beijing Institute of Technology, Beijing 100081, China (e-mail: hhu@bit.edu.cn); H. Shan is with the College of Information Science and Electronic Engineering, Zhejiang University, Hangzhou 310027, China, and also with Zhejiang Provincial Key Laboratory of Information Processing, Communication and Networking, Hangzhou, China (e-mail: hshan@zju.edu.cn); T. Q. S. Quek is with the Singapore University of Technology and Design, Singapore 487372, and also with the Yonsei Frontier lab, Yonsei University, South Korea (e-mail: tonyquek@sutd.edu.sg); P. Zhao is with the School of Cyber Science and Technology, Sun Yat-Sen University, Shenzhen 518107, China. (e-mail: zhaopn@mail.sysu.edu.cn).

as a promising solution for this dilemma [6]. In FL, model training is completed by exchanging something about model parameters, such as the model parameter itself or the gradient of the loss function with respect to model parameters, between each involving user and one central server iteratively. In each round of iteration, the central server aggregates the model parameters from every user and subsequently broadcasts the aggregated one to all the users. After receiving the broadcasted model parameter, each user performs the role of local updating based on its own data. In such a procedure, there is no exchange of raw data between any user and the central server [7], [8].

However, distributed training paradigms such as FL inherently encounter robustness challenges stemming from the participation of multiple heterogeneous users. To be specific, due to data corruption, device malfunctioning, or malicious attacks at some users, the information about the model parameter to be uploaded to the central server by these abnormal users may deviate from the expected one [9], [10]. In such a case, the group of abnormal users are called as Byzantine users, and the action of Byzantine users is referred to as Byzantine attacks [11], [12]. As a comparison, the group of normal users are called as *Honest users*. For a Byzantine attack, it is general to assume the uncertainty of the identity and the population of Byzantine users. What is more, the attack initiated by Byzantine users could be arbitrarily malicious [13], [14]. With such a setup, the training performance of FL will be surely degraded and aggregation strategies resistant to Byzantine attacks have been concerned in literature [15].

On the other hand, the training process of FL faces challenges of data heterogeneity among users. This heterogeneity comes from the diverse distribution of local data, as the local data may be collected by each FL user in their specific environmental conditions, habits, or preferences [16]. In such a case, data distributions over multiple users are always assumed to be non independently and identically distributed (non-IID). The presence of data heterogeneity has already been demonstrated to cause local drift of user model, and thus, degradation of the global model's performance. How to be adaptive to data heterogeneity is also an important issue and has been studied extensively in the area of FL [17].

A. Related Works

In the field of FL, numerous studies have considered a wide range of factors. However, research on aggregation strategies that are robust to Byzantine attacks in association with rigorous convergence analysis remains limited, primarily due to the significant challenges such attack introduces into the aggregation process. The system assumptions, which serve as an essential precondition for convergence analysis, usually relate to the nature of the data (IID or non-IID), the nature of the loss function (strongly-convex or non-convex), and the way of local updating (one-step or multiple steps), etc. For these assumptions, the data heterogeneity and non-convex loss function make FL framework more general, and multiple steps of local updating waives each user from frequent communication with the central server. The Byzantine-resilient aggregation strategies in the literature of FL under diverse system assumptions have been summarized in Table I.

As of the aggregation strategies in related literature, by leveraging median [15] or iterative filtering [21], the associated FL system can tolerate a small fraction of Byzantine users. To be more robust to Byzantine attacks, some methods such as trimmed mean [18], Robust Aggregating Normalized Gradient Method (RANGE) [19], a Huber Loss Minimization [20], semi verified mean estimation [22], Krum [23], Best Effort Voting SGD (BEV-SGD) [24], Robust Stochastic Aggregation (RSA) [25], Maximum Correntropy Aggregation (MCA) [26], Self-Driven Entropy Aggregation (SDEA) [30], and Robust Accumulated Gradient Estimation (RAGE) [31] have been proposed. Specifically, [18] aggregates the upload vectors by calculating their coordinate-wise median or coordinate-wise trimmed mean based on [15]. RANGE takes the median of uploaded vectors from each client as the aggregated one, and each uploaded vector is supposed to be the median of the previously transmitted gradients. [20] improve the trimmed mean on non-IID datasets by utilizing a multi-dimensional Huber loss function to aggregate uploaded vectors. [22] utilizes semiverified mean estimation to filter out vectors from Byzantine attackers before aggregation, building on the iterative filtering method. Krum [23] selects a stochastic gradient as the global one, knowing the number of Byzantine attackers, by choosing the gradient with the shortest cumulative distance from a group of the most closely distributed stochastic gradients, BEV-SGD [24] requires each user to normalize the associated local gradient to be a vector with zero mean and unit variance before offloading it to the central server, RSA [25] penalizes the difference between local model parameters and global model parameters to isolate Byzantine users, while MCA [26] utilizes its the maximum correntropy of the model parameters' distribution characteristics and compute the central value to update the global model parameter. Moreover, the SDEA method [30] partially leverages a public dataset to enhance global model training and mitigate Byzantine attacks, with its effectiveness validated through empirical experiments. In contrast, the RAGE approach [31] enables multiple local gradient updates under heterogeneous data distributions. While theoretically well-founded, this method assumes that the Byzantine ratio, i.e., the proportion of malicious participants, remains below one-third.

Although the above aggregation strategies can be somewhat resistant to Byzantine attacks at some extent, some of them may still fail to work in front of heavy Byzantine attacks [32], [33]. Recently, the geometric median has emerged as a promis-

ing candidate for aggregation due to its ability to naturally tolerate a larger fraction of strong Byzantine attacks without any additional conditions [34]. Based on geometric median, some algorithms such as Robust Federated Aggregation (RFA) [27], Byzantine attack resilient distributed Stochastic Average Gradient Algorithm (Byrd-SAGA) [28], and Byzantine-RObust Aggregation with gradient Difference Compression And STochastic variance reduction (BROADCAST) [29], have been proposed. To be specific, geometric median is leveraged to aggregate the uploaded vectors for RFA, Byrd-SAGA, and BROADCAST. Differently, each user in RFA selects the trimmed mean of the model parameters over multiple local updating as the uploaded vector, while Byrd-SAGA and BROADCAST utilize the SAGA [35] method to generate the vectors for aggregation first and then upload them in a lossless or compressive way.

In the aforementioned geometric median aggregation strategies, there has been little work claiming to be adaptive to data heterogeneity, though this remains a non-negligible issue. RFA in [27] is an exception. However, RFA only investigates strongly-convex loss function. With such a convexity setup, RFA shows that it is can converge to a neighborhood of the optimal solution only if the number of local updates for each involving user is larger than then a threshold so as to fulfill a necessary inequality. However, this restricts the flexibility of selecting the number of local updates and maybe computationally intensive when these users have limited computation capability.

B. Motivations and Contributions

In this paper we investigate Byzantine-resilient FL with adaptivity to data heterogeneity, which was only studied in [25], [26], [27], [30], and [31], referred to as RSA, MCA, RFA, SDEA, and RAGE, respectively. Different from RSA, MCA, and RFA, which merely considers strongly-convex loss function, we investigate not only strongly-convex but also non-convex loss function. Specifically, in departure from RFA, which also uses geometric median for aggregation but has a convergence condition that necessitates local update steps exceeding a theoretically established threshold, our architecture introduces a flexible round number of local updates scheme, thereby eliminating this fundamental constraint while maintaining convergence guarantees.

While SDEA is effective in practice, it lacks a formal theoretical convergence analysis and depends on the availability of public data, which may not always be practical or feasible. In contrast to SDEA, our approach does not assume access to any public data and provides rigorous theoretical guarantees. Moreover, unlike RAGE, which requires the Byzantine ratio to be no greater than one-third, our method can tolerate a higher Byzantine ratio, potentially approaching one-half. With our featured system setup, we propose a novel FL structure, RAGA. Specifically, the RAGA leverages the geometric median to aggregate the local gradients offloaded by the users after multiple rounds of local updating. Associated analysis of convergence and robustness are then followed for both non-convex and strongly-convex loss functions. Our main contributions are summarized as follows:

References	Algorithm	Function Type	Data Heterogeneity	Local Updating	Optimality Gap	
[15]	median	-	IID	one step	-	
[18]	trimmed mean	non-convex strongly-convex	IID	one step	non-zero	
[19]	RANGE	non-convex strongly-convex	IID	one step	non-zero	
[20]	-	non-convex strongly-convex	little data heterogeneity	one step	non-zero	
[21]	iterative filtering	strongly-convex	IID	one step	non-zero	
[22]	-	strongly-convex	IID	one step	non-zero	
[23]	Krum	non-convex	IID	one step	non-zero	
[24]	BEV-SGD	non-convex	IID	one step	zero	
[25]	RSA	strongly-convex	non-IID	one step	non-zero	
[26]	MCA	strongly-convex	non-IID	one step	non-zero	
[27]	RFA	strongly-convex	non-IID	multiple steps	non-zero	
[28]	Byrd-SAGA	strongly-convex	IID	one step	non-zero	
[29]	BROADCAST	strongly-convex	IID	one step	non-zero	
[30]	SDEA	-	non-IID	multiple steps	-	
[31]	RAGE	non-convex strongly-convex	non-IID	multiple steps	non-zero	
This work	RAGA	non-convex	non-IID	multiple steps	non-zero	

TABLE I: List of references on the convergence of FL under Byzantine attacks.

Algorithmically, we propose a new FL aggregation strategy, named RAGA, which has the flexibility of arbitrary selection of local update's step number, and is robust to both Byzantine attack and data heterogeneity, and does not rely on the use of a public dataset.

strongly-convex

- Theoretically, we establish a convergence guarantee for our proposed RAGA under not only non-convex but also strongly-convex loss function. Through rigorous proof, we show that the established convergence can be promised as long as the fraction of dataset from Byzantine users is less than half. The achievable convergence rate can be at $\mathcal{O}(1/T^{2/3-\delta})$ where T is the iteration number and $\delta \in (0,2/3)$ for non-convex loss function, and at linear for strongly-convex loss function. Moreover, stationary point and global optimal solution are shown to be obtainable as data heterogeneity, algorithmic error, and stochastic local gradient variance diminish, for non-convex and strongly-convex loss function, respectively.
- Empirically, we conduct extensive experiments to evaluate the performance of our proposed RAGA. With non-IID dataset, our proposed RAGA is verified to be robust to various Byzantine attack types and ratios. Moreover, compared with baseline methods, our proposed RAGA can achieve higher test accuracy.

C. Organization and Notation

The rest of this paper is organized as follows: Section II introduces the system model and formulates the problem to be solved in this paper, Section III presents our proposed RAGA. In Section IV, the analysis of convergence and robustness for our proposed RAGA under non-convex and strongly-convex loss function are disclosed. Experimental results are illustrated in Section V, followed by conclusion remarks in Section VI.

Notation: We use plain and bold letters to represent scalars and vectors respectively, e.g., a and b are scalars, x and y are vectors. $\langle x, y \rangle$ denotes the inner product of the vectors x and y, $\nabla F(x_0)$ represents the gradient vector of function F(x) at $x = x_0$, ||x|| stands for the Euclidean norm $||x||_2$, $\mathbb{E}\{a\}$ and $\mathbb{E}\{x\}$ implies the expectation of random variable a and random vector x respectively, and $a \propto b$ means that a is proportional to b.

II. PROBLEM STATEMENT

Consider a FL system with one central server and M users, which composite the set $\mathcal{M} \triangleq \{1,2,...,M\}$. At the side of mth user, it has a dataset \mathcal{S}_m , which has S_m ground-true labels. In the FL system, the learning task is to train a model parameter $\boldsymbol{w} \in \mathbb{R}^p$ to minimize the global loss function,

denoted as F(w), for approximating the data labels of all the users. Specifically, we need to solve the following problem *Problem 1:*

$$\min_{\boldsymbol{w}\in\mathbb{R}^p}F(\boldsymbol{w}).$$

In Problem 1, the global loss function F(w) is defined as

$$F(\boldsymbol{w}) \triangleq \frac{1}{\sum_{m \in \mathcal{M}} S_m} \sum_{m \in \mathcal{M}} \sum_{\boldsymbol{s} \in S_m} f(\boldsymbol{w}, \boldsymbol{s}), \tag{1}$$

where f(w, s) denotes the loss function for data sample s. For convenience, we define the local loss function of mth user as

$$F_m(\boldsymbol{w}) \triangleq \frac{1}{S_m} \sum_{\boldsymbol{s} \in S_m} f(\boldsymbol{w}, \boldsymbol{s}),$$
 (2)

then the global loss function F(w) can be rewritten as

$$F(\boldsymbol{w}) = \sum_{m \in \mathcal{M}} \frac{S_m}{\sum_{i \in \mathcal{M}} S_i} F_m(\boldsymbol{w}).$$
(3)

In traditional FL, iterative interactions between a group of M users and a central server are performed to update the gradient parameter $\nabla F(\boldsymbol{w})$ until convergence. For tth round of iteration, a conventional operation procedure can be given as the following steps:

Step 1 (Local Update): For mth user, it calculates the local gradient parameter $\nabla F_m(\boldsymbol{w}^t)$ from its local dataset \mathcal{S}_m and global model parameter \boldsymbol{w}^t .

Step 2 (Aggregation and Broadcasting): Each user sends its local gradient parameter $\nabla F_m(\boldsymbol{w}^t)$ to the central server. The central server then aggregates all the local gradient vectors into a common one, denoted as \boldsymbol{w}^{t+1} , as follows,

$$\boldsymbol{w}^{t+1} = \boldsymbol{w}^t - \eta \cdot \sum_{m=1}^{M} \nabla F_m(\boldsymbol{w}^t), \tag{4}$$

then the central server broadcasts w^{t+1} to all the users.

With some combination of previously claimed assumptions, the above iterative operation may help to reach the optimal or convergent solution of Problem 1 if each user sends trustworthy message to the central server. However, under Byzantine attacks, the main challenge of solving Problem 1 comes from the fact that the Byzantine attackers can collude and send arbitrary malicious messages to the central server so as to bias the optimization process. We aspire to develop a robust FL algorithm to address this issue in next section.

III. PROPOSED AGGREGATION STRATEGY: ROBUSTNESS AVERAGE GRADIENT ALGORITHM (RAGA)

Before the introduction of the RAGA, we first explain the scenario of Byzantine attack. Assume there are B Byzantine users out of M users, which compose the set of \mathcal{B} . Any Byzantine user can send an arbitrary vector $\star, \star \in \mathbb{R}^p$ to the central server. Suppose z_m^t is the real vector uploaded by mth user to the central server in tth round of iteration, then there is

$$\boldsymbol{z}_{m}^{t} = \begin{cases} \boldsymbol{g}_{m}^{t}, & m \in \mathcal{M} \setminus \mathcal{B} \\ \star, & m \in \mathcal{B} \end{cases}, \tag{5}$$

where g_m^t denotes the vector to be uploaded by honest user $(m \in \mathcal{M} \setminus \mathcal{B})$. Additionally, we also assume $\sum_{m \in \mathcal{B}} S_m < \infty$

 $\frac{1}{2}\sum_{m\in\mathcal{M}}S_m$. In related works [28], by implicitly supposing S_m to be identical for every $m\in\mathcal{M}$, it is usually assumed $B<\frac{1}{2}M$, which is a special realization of our assumption.

To reduce communication burden due to frequent interactions between M users and the central server and overcome the Byzantine attacks, we propose the RAGA, which runs multi-local updates and aggregates all the uploaded vectors in a robust way. Specifically, in tth round of iteration:

Step 1 (Multi-Local Update): For any honest user $m, m \in \mathcal{M} \setminus \mathcal{B}$. Denote $\boldsymbol{w}_m^{t,k}$ as the local model parameter of mth user for kth update and $\eta_m^{t,k}$ as the associated learning rate. By implementing stochastic gradient descend (SGD) method, there is

$$\mathbf{w}_{m}^{t,k} = \mathbf{w}_{m}^{t,k-1} - \eta_{m}^{t,k} \cdot \nabla F_{m}(\mathbf{w}_{m}^{t,k-1}; \xi_{m}^{t,k}),$$

$$k = 1, 2, \dots, K^{t},$$
(6)

where $\xi_m^{t,k}$ is a randomly selected subset of dataset \mathcal{S}_m and $\boldsymbol{w}_m^{t,0} = \boldsymbol{w}^t$. The \boldsymbol{w}^t is received from t-1 round of iteration. Specially, for the sake of robustness and convergence, we set

$$oldsymbol{z}_m^t = oldsymbol{g}_m^t = rac{1}{K^t} \sum_{k=1}^{K^t}
abla F_m(oldsymbol{w}_m^{t,k-1}; \xi_m^{t,k}) ext{ for } m \in \mathcal{M} \setminus \mathcal{B}.$$

Step 2 (Aggregation and Broadcasting): For the mth user, it uploads its own vector \boldsymbol{z}_m^t to the central server for $m \in \mathcal{M}$. To ensure the robustness of the FL system, we use the numerical geometric median of all the uploaded vectors, which is defined as

$$\boldsymbol{w}^{t+1} = \boldsymbol{w}^t - \boldsymbol{\eta}^t \cdot \boldsymbol{z}^t, \tag{7}$$

where η^t represents the global learning rate for tth round of iteration and \boldsymbol{z}^t represents the numerical estimation of the geometric median of $\{\boldsymbol{z}_m^t|m\in\mathcal{M}\}$, i.e., geomed $(\{\boldsymbol{z}_m^t|m\in\mathcal{M}\})$. The geomed $(\{\boldsymbol{z}_m^t|m\in\mathcal{M}\})$ in this paper is defined as

$$\boldsymbol{z}^{t,*} \triangleq \operatorname{geomed}\left(\left\{\boldsymbol{z}_{m}^{t} \middle| m \in \mathcal{M}\right\}\right)$$

$$= \arg\min_{\boldsymbol{y}} \sum_{i=1}^{M} \frac{S_{i}}{\sum_{i=1}^{M} S_{i}} \left\|\boldsymbol{y} - \boldsymbol{z}_{i}^{t}\right\|. \tag{8}$$

The problem in (8) is actually a convex optimization problem and an ϵ -optimal solution is obtainable by resorting to Weiszfeld algorithm [36]. Hence the z^t fulfills the following condition

$$\sum_{i=1}^{M} \frac{S_i}{\sum_{j=1}^{M} S_j} \| \boldsymbol{z}^t - \boldsymbol{z}_i^t \| \leqslant \sum_{i=1}^{M} \frac{S_i}{\sum_{j=1}^{M} S_j} \| \boldsymbol{z}^{t,*} - \boldsymbol{z}_i^t \| + \epsilon,$$
(9)

and is also denoted as geomed $(\{z_m^t|m\in\mathcal{M}\},\epsilon)$ in the sequel. Then the central server broadcasts the global model parameter \boldsymbol{w}^{t+1} to all the users for preparing the calculation in t+1 round of iteration.

Based on the above description, the RAGA is conceptually illustrated in Fig 1 and summarized in Algorithm 1.

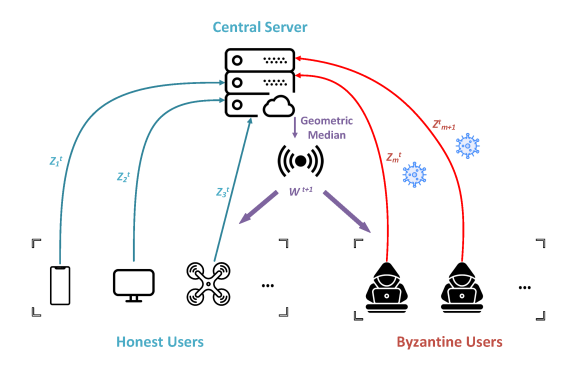


Fig. 1: Illustration of Byzantine-resilient RAGA FL system.

Algorithm 1: The procedure of RAGA.

1 The central server initializes the model parameter w^1 and sends it to all the users.

```
2 for t = 1, 2, ..., T do
               for m \in \mathcal{M} \setminus \mathcal{B} do
 3
                        Set \boldsymbol{w}_m^{t,0} = \boldsymbol{w}^t.
for k = 1, 2, \dots, K^t do
  4
  5
                                  Randomly select local data subset \xi_m^{t,k} from
  6
                                     \begin{aligned} &\mathcal{S}_m \text{ and set} \\ &\boldsymbol{w}_m^{t,k} = \boldsymbol{w}_m^{t,k-1} - \eta_m^{t,k} \nabla F_m(\boldsymbol{w}_m^{t,k-1}; \boldsymbol{\xi}_m^{t,k}). \end{aligned} 
  7
                       Set \boldsymbol{z}_m^t = \frac{1}{K^t} \sum_{k=1}^{K^t} \nabla F_m(\boldsymbol{w}_m^{t,k-1}; \boldsymbol{\xi}_m^{t,k}).
  8
               end
 9
               for m \in \mathcal{B} do
10
                         Set z_m^t = \star.
11
12
               All the users send their own z_m^t to the central
13
               server. The central server obtains the geometric
                \begin{array}{l} \text{median } \boldsymbol{z}^t = \text{geomed} \left( \{ \boldsymbol{z}_m^t | m \in \mathcal{M} \}, \epsilon \right) \text{, updates} \\ \boldsymbol{w}^{t+1} = \boldsymbol{w}^{t} - \boldsymbol{\eta}^t \cdot \boldsymbol{z}^t \text{, and then broadcasts} \\ \end{array} 
               \boldsymbol{w}^{t+1} to all the users.
14 end
```

IV. ANALYSIS OF CONVERGENCE AND ROBUSTNESS

In this section, we provide theoretical analysis of the robustness and convergence of the RAGA under Byzantine attacks under two cases of loss function's convexity. Below, we first present the necessary assumptions.

A. Assumption

For all honest users $m \in \mathcal{M} \setminus \mathcal{B}$, we have the following assumptions.

Assumption 1 (Lipschitz Continuity): The loss function f(w, s) has L-Lipschitz continuity [37], [38], i.e., for $\forall w_1, w_2 \in \mathbb{R}^p$, there is

$$f(\boldsymbol{w}_{1}, \boldsymbol{s}) - f(\boldsymbol{w}_{2}, \boldsymbol{s}) \leqslant \langle \nabla f(\boldsymbol{w}_{2}, \boldsymbol{s}), \boldsymbol{w}_{1} - \boldsymbol{w}_{2} \rangle + \frac{L}{2} \|\boldsymbol{w}_{1} - \boldsymbol{w}_{2}\|^{2}, \quad (10)$$

which is equivalent to the following inequality,

$$\|\nabla f(\mathbf{w}_1, \mathbf{s}) - \nabla f(\mathbf{w}_2, \mathbf{s})\| \le L \|\mathbf{w}_1 - \mathbf{w}_2\|.$$
 (11)

With (30) or (31), it can be derived that the global loss function F(w) and local loss function $F_m(w)$ both have L-Lipschitz continuity.

Assumption 2 (Strongly-Convex): The loss function $f(\boldsymbol{w}, \boldsymbol{s})$ is μ strongly-convex [37], i.e., for $\forall \boldsymbol{w}_1, \boldsymbol{w}_2 \in \mathbb{R}^p$, there is

$$\|\nabla f(\mathbf{w}_1, \mathbf{s}) - \nabla f(\mathbf{w}_2, \mathbf{s})\| \ge \mu \|\mathbf{w}_1 - \mathbf{w}_2\|.$$
 (12)

Similarly, with (32), F(w) and $F_m(w)$ can be derived to be both μ strongly-convex.

Assumption 3 (Local Unbiased Gradient): Suppose a subset of dataset S_m is selected randomly, which is denote as ξ_m , define

$$F_m(\boldsymbol{w}; \xi_m) \triangleq \frac{1}{|\xi_m|} \sum_{\boldsymbol{s} \in \mathcal{E}_m} f(\boldsymbol{w}, \boldsymbol{s}),$$
 (13)

the unbiased gradient [37], [38] implies that

$$\mathbb{E}\left\{\nabla F_m(\boldsymbol{w}; \boldsymbol{\xi}_m)\right\} = \nabla F_m(\boldsymbol{w}). \tag{14}$$

Assumption 4 (Bounded Inner Variance): For each honest user m and $\mathbf{w} \in \mathbb{R}^p$, the variance of stochastic local gradient $\nabla F_m(\mathbf{w}; \xi_m)$ is upper-bounded [37], [38] by

$$Var(\nabla F_m(\boldsymbol{w}; \xi_m)) \leqslant \sigma^2. \tag{15}$$

Assumption 5 (Data Heterogeneity): For each honest user m and $w \in \mathbb{R}^p$, the data heterogeneity can be defined as

$$\theta_m = \|\nabla F_m(\boldsymbol{w}) - \nabla F(\boldsymbol{w})\|. \tag{16}$$

We also assume the data heterogeneity is bounded [37], [38], which implies

$$\theta_m \leqslant \theta.$$
 (17)

Assumption 6 (Bounded Gradient): For each honest user m and $\mathbf{w} \in \mathbb{R}^p$, the ideal local gradient $\nabla F_m(\mathbf{w})$ is upperbounded [37], [38] by

$$\|\nabla F_m(\boldsymbol{w})\| \leqslant G. \tag{18}$$

B. Convergence Analysis

In this subsection, we present the analytical results of convergence on our proposed RAGA. All proofs are deferred to Appendices B and C.

1) Case I: With Lipschitz Continuity Only for Loss Function: We first inspect the case with Assumptions 7, 9, 10, 11 and 12 imposed, which allows the loss function to be nonconvex. By defining

$$\alpha_m = \frac{S_m}{\sum_{j=1}^M S_j}, C_\alpha = \sum_{m \in \mathcal{M} \setminus \mathcal{B}} \alpha_m, \tag{19}$$

and

$$p^{t} = \begin{cases} 0, & \eta^{t} \leqslant \frac{1}{L} \\ 1, & \eta^{t} > \frac{1}{L} \end{cases}$$
 (20)

the following results can be expected.

Theorem 1: With $C_{\alpha} > 0.5$, there is

$$\sum_{t=1}^{T} \frac{\eta^{t}}{\sum_{t'=1}^{T} \eta^{t'}} \mathbb{E}\left\{ \left\| \nabla F(\boldsymbol{w}^{t}) \right\|^{2} \right\} \\
\leq \frac{2\mathbb{E}\left\{ F(\boldsymbol{w}^{1}) - F(\boldsymbol{w}^{T}) \right\}}{\sum_{t'=1}^{T} \eta^{t'}} + \frac{1}{\sum_{t'=1}^{T} \eta^{t'}} \sum_{t=1}^{T} \eta^{t} \Delta^{t} \\
+ \sum_{t=1}^{T} \frac{2(\eta^{t} + p^{t}(\eta^{t})^{2}L - p^{t}\eta^{t})\epsilon^{2}}{(2C_{\alpha} - 1)^{2} \sum_{t'=1}^{T} \eta^{t'}} \\
+ \sum_{t=1}^{T} \frac{8(C_{\alpha})^{2}(\eta^{t}\sigma^{2} + (p^{t}(\eta^{t})^{2}L - p^{t}\eta^{t})(G^{2} + \sigma^{2}))}{(2C_{\alpha} - 1)^{2} \sum_{t'=1}^{T} \eta^{t'}}, \tag{21}$$

where

$$\Delta^{t} = \frac{8C_{\alpha}}{(2C_{\alpha} - 1)^{2}} \sum_{m \in \mathcal{M} \setminus \mathcal{B}} \left(\frac{2\alpha_{m}L^{2}(G^{2} + \sigma^{2})}{K^{t}} \sum_{k=2}^{K^{t}} (k - 1) \cdot \sum_{i=1}^{k-1} (\eta_{m}^{t,i})^{2} + 2\alpha_{m}\theta^{2} \right).$$
(22)

Proof: Please refer to Appendix B.

Remark 1:

• In general case, when $\lim_{T \to \infty} \sum_{t=1}^{T} \eta^t = \infty$,

$$\lim_{T \to \infty} \sum_{t=1}^{T} \eta^t \sum_{m \in \mathcal{M} \setminus \mathcal{B}} \sum_{i=1}^{K^t} (\eta_m^{t,i})^2 < \infty, \text{ and there are only finitely many } t \text{ such that } p^t = 1, \text{ together with the prerequisite condition of Theorem 3, i.e., } C_\alpha > 0.5, \text{ it can be derived that the term } \sum_{t=1}^{T} \frac{\eta^t}{\sum_{t'=1}^{T} \eta^t} \mathbb{E} \left\{ \left\| \nabla F(\boldsymbol{w}^t) \right\|^2 \right\}$$

will converge to $\mathcal{O}\left(\theta^2 + \epsilon^2 + \sigma^2\right)$.

• To be concrete, we set $\eta_m^{t,k} = \eta^t \leqslant \frac{1}{L}$ and $K^t = K$. Then inequality (41) dwells into

$$\sum_{t=1}^{T} \frac{\eta^{t}}{\sum_{t'=1}^{T} \eta^{t}} \mathbb{E} \left\{ \left\| \nabla F(\boldsymbol{w}^{t}) \right\|^{2} \right\}
\leq \frac{8(C_{\alpha})^{2} L^{2}(G^{2} + \sigma^{2})(K - 1)(2K - 1) \sum_{t=1}^{T} (\eta^{t})^{3}}{3(2C_{\alpha} - 1)^{2} \sum_{t=1}^{T} \eta^{t}}
+ \frac{2\mathbb{E} \left\{ F(\boldsymbol{w}^{1}) - F(\boldsymbol{w}^{T}) \right\}}{\sum_{t=1}^{T} \eta^{t}} + \frac{16(C_{\alpha})^{2} \theta^{2} + 2\epsilon^{2} + 8(C_{\alpha})^{2} \sigma^{2}}{(2C_{\alpha} - 1)^{2}}, \tag{23}$$

which will converge to

$$\frac{16(C_{\alpha})^2}{(2C_{\alpha}-1)^2}\theta^2 + \frac{2}{(2C_{\alpha}-1)^2}\epsilon^2 + \frac{8(C_{\alpha})^2}{(2C_{\alpha}-1)^2}\sigma^2, \tag{24}$$

as long as
$$\lim_{T \to \infty} \sum_{t=1}^{T} (\eta^t)^3 < \infty$$
.

• To further concrete convergence rate, we set $\eta^t = \frac{\eta_0}{L} \frac{1}{(t+c)^{1/3+\delta}}$, where δ is an arbitrary value lying between (0,2/3), $\eta_0 < 1$ and c > 0, the right shift introduced by adding c > 0 to the denominator is

intended to mitigate fluctuations during the initial training iterations, then the right-hand side of (21) of the revised manuscript is upper bounded by

$$\mathcal{O}\left(\frac{8\eta_0^2(C_{\alpha})^2(G^2 + \sigma^2)(K - 1)(2K - 1)(1 + 3\delta - 3\delta T^{-3\delta})}{3(2C_{\alpha} - 1)^2 T^{2/3 - \delta}}\right) + \mathcal{O}\left(\frac{2L\mathbb{E}\left\{F(\boldsymbol{w}^1) - F(\boldsymbol{w}^T)\right\}}{\eta_0 T^{2/3 - \delta}}\right) + \frac{16(C_{\alpha})^2 \theta^2 + 2\epsilon^2 + 8(C_{\alpha})^2 \sigma^2}{(2C_{\alpha} - 1)^2}, \tag{25}$$

which still converges to the result in (24) at rate $\mathcal{O}\left(\frac{1}{T^{2/3-\delta}}\right)$. From previous inference from Theorem 3, it can be found

- From previous inference from Theorem 3, it can be found that the minimum of $\mathbb{E}\left\{\left\|\nabla F(\boldsymbol{w}^t)\right\|^2\right\}$ over $t\in[1,T]$, which is upper bounded by the left-hand side of (41), and thus the expression in (24). The non-zero gap shown in (24) will vanish as θ , ϵ and σ , which represent data heterogeneity, error tolerance to numerically work out the geometric median through Weiszfeld algorithm, and the variance of stochastic local gradient respectively, go to zero. In other words, once the \mathcal{S}_m among $m\in\mathcal{M}$ are IID, \mathcal{S}_m for every $m\in\mathcal{M}$ are fully utilized to calculate local gradient, and the geometric median is calculated perfectly, there will be one $\nabla F(\boldsymbol{w}^t)$ for $t\in[1,T]$ being zero, which implies the reaching of stationary point for Problem 1.
- Last but not least, the above convergence results are based on the assumption that $C_{\alpha} > 0.5$, i.e., the fraction of the datasets from Byzantine attackers is less than half, which shows a strong robustness to Byzantine attacks.
- 2) Case II: With Lipschitz Continuity and Strong Convexity for Loss Function: For the case with Assumptions 7, 8, 9, 10, 11 and 12 imposed, which requires the loss function to be not only Lipschitz but also strongly-convex, the following results can be anticipated.

Theorem 2: With $0 < \lambda^t < 1$ and $C_{\alpha} > 0.5$, the optimality gap $\mathbb{E}\left\{F(\boldsymbol{w}^T) - F(\boldsymbol{w}^*)\right\}$ is upper bounded in (43) as follows.

$$\mathbb{E}\left\{F(\boldsymbol{w}^{T}) - F(\boldsymbol{w}^{*})\right\}
\leq \frac{L}{2}\mathbb{E}\left\{\left\|\boldsymbol{w}^{1} - \boldsymbol{w}^{*}\right\|^{2}\right\} \prod_{t=1}^{T-1} \gamma^{t} + \frac{L}{2} \sum_{t=1}^{T-1} \frac{(\eta^{t})^{2}}{\lambda^{t}} \left(\Delta^{t} + \frac{8\sigma^{2}(C_{\alpha})^{2}}{(2C_{\alpha} - 1)^{2}} + \frac{2\epsilon^{2}}{(2C_{\alpha} - 1)^{2}}\right) \cdot \prod_{i=t}^{T-1} (\gamma^{i+1})^{q^{i+1}}, \quad (26)$$

where

$$q^t = \begin{cases} 0, & t = T \\ 1, & t < T \end{cases},$$

and

$$\gamma^t = \frac{1 - 2\eta^t \mu + L^2(\eta^t)^2}{1 - \lambda^t}.$$

Proof: Please refer to Appendix C.

Remark 2:

• For general case, as long as $\eta_m^{t,k} \propto T^{-\beta}, \beta > 0$, $\lambda^t = \rho^t \eta^t$ with $\rho^t < 2\mu$ and $\eta^t < \frac{2\mu - \rho^t}{L^2}$, $0 < \gamma^t < 1$,

and the preconditions listed in Theorem 4 hold, the convergence of our proposed RAGA can be ensured and the optimality gap is at the scale $\mathcal{O}\left(\theta^2 + \epsilon^2 + \sigma^2\right)$.

• To concrete the optimality gap, we suppose $\eta_m^{t,k} = \frac{1}{T}\eta$, $\eta^t = \eta, \ \gamma^t = \gamma, \ K^t = K, \ \lambda^t = \mu \eta^t = \mu \eta, \ \text{and} \ \eta^t < \frac{\mu}{L^2},$

$$\mathbb{E}\left\{F(\boldsymbol{w}^{T}) - F(\boldsymbol{w}^{*})\right\}
\leq \frac{L(\gamma)^{T-1}}{2} \mathbb{E}\left\{\left\|\boldsymbol{w}^{1} - \boldsymbol{w}^{*}\right\|^{2}\right\}
+ \frac{4L^{3}(K-1)(2K-1)(C_{\alpha})^{2}(G^{2} + \sigma^{2})}{3\mu(2C_{\alpha} - 1)^{2}T^{2}} \frac{1 - (\gamma)^{T}}{1 - \gamma}(\eta)^{3}
+ \frac{8L(C_{\alpha})^{2}\theta^{2} + \epsilon^{2}L + 4L(C_{\alpha})^{2}\sigma^{2}}{\mu(2C_{\alpha} - 1)^{2}} \frac{1 - (\gamma)^{T}}{1 - \gamma}\eta. \tag{27}$$

When $T \rightarrow \infty$, $(\gamma)^{T-1} \rightarrow 0$ and $\frac{1-(\gamma)^T}{1-\gamma} \rightarrow$ $\frac{1}{1-\gamma} = \frac{1-\mu\eta}{\mu\eta - L^2(\eta)^2} < \infty. \text{ Therefore, } \frac{1-\gamma}{T^2(1-\gamma)} \xrightarrow{7} \frac{1-(\gamma)^T}{T^2(1-\gamma)} \rightarrow \frac{1-\eta}{1-\mu\eta}$ $\frac{1-\mu\eta}{T^2(\mu\eta-L^2(\eta)^2)} \to 0 \text{ and } \frac{\eta(1-(\gamma)^T)}{1-\gamma} \to \frac{1-\mu\eta}{\mu-L^2\eta}$ In this case, $\mathbb{E}\left\{F(\boldsymbol{w}^T)-F(\boldsymbol{w}^*)\right\}$ will converge to

$$\frac{1 - \mu \eta}{\mu - L^2 \eta} \left(\frac{8L(C_{\alpha})^2}{\mu (2C_{\alpha} - 1)^2} \theta^2 + \frac{L}{\mu (2C_{\alpha} - 1)^2} \epsilon^2 + \frac{4L(C_{\alpha})^2}{\mu (2C_{\alpha} - 1)^2} \sigma^2 \right), \quad (28)$$

at a rate
$$\mathcal{O}\left((\gamma)^{T-1} + \frac{1}{T^2}\right)$$
.

at a rate $\mathcal{O}\left((\gamma)^{T-1}+\frac{1}{T^2}\right)$.

• To further concrete convergence rate, we alternatively set $\eta_m^{t,k}=(TK)^{-\beta}\eta$ with $\beta>0$, then the optimality gap of (43) can be bounded by

$$\left(\frac{4L^{3}(K-1)(2K-1)(C_{\alpha})^{2}(G^{2}+\sigma^{2})}{3\mu(2C_{\alpha}-1)^{2}(TK)^{2\beta}}\frac{1-(\gamma)^{T}}{1-\gamma}(\eta)^{3}\right) + \left(\frac{L(\gamma)^{T-1}}{2}\mathbb{E}\left\{\left\|\boldsymbol{w}^{1}-\boldsymbol{w}^{*}\right\|^{2}\right\}\right) + \frac{8L(C_{\alpha})^{2}\theta^{2}+\epsilon^{2}L+4L(C_{\alpha})^{2}\sigma^{2}}{\mu(2C_{\alpha}-1)^{2}}\frac{1-(\gamma)^{T}}{1-\gamma}\eta, \tag{29}$$

which also convergences to (28) but at a rate $\mathcal{O}\left((\gamma)^{T-1}+(TK)^{-2\beta}\right)$. This rate can be adjusted by β and would be linear when $\beta \propto T$.

- Compared with the discussion in Remark 1 that works for non-convex loss function, we can obtain zero optimality gap as θ , ϵ , and σ go to zero for strongly-convex loss function in this case, which implies the achievement of global optimal solution rather than stationary point as in Remark 1. Moreover, linear convergence rate is achievable in this case and is faster than the rate $\mathcal{O}\left(\frac{1}{T^{2/3-\delta}}\right)$ as shown in Remark 1.
- It is also worthy to note that the above results still hold on the condition that $C_{\alpha} > 0.5$, which promises a strong robustness to Byzantine attacks.

V. EXPERIMENTS

In this section, we conduct experiments to inspect the convergence performance of our proposed RAGA under various system setups together with baseline methods, so as to verify the advantage of RAGA over peers in being robust to Byzantine attacks in front of heterogeneous dataset.

A. Setup

To carry out experiments, we set up a machine learning environment in PyTorch 2.3.1 on Ubuntu 20.04, powered by two 3090 GPUs and two Intel Xeon Gold 6226R CPUs.

Datasets:

- MNIST: MNIST dataset includes a training set and a test set. The training set contains 60000 samples and the test set contains 10000 samples, each sample of which is a 28×28 pixel grayscale image.
- **CIFAR10:** The CIFAR10 dataset includes a training set and a test set. The training set contains 50,000 samples, and the test set contains 10,000 samples, each of which is a 32×32 pixel color image.
- CIFAR100: The CIFAR100 dataset includes a training set and a test set. The training set contains 50,000 samples, and the test set contains 10,000 samples, each of which is a 32×32 pixel color image.

We split the above three datasets into M non-IID training sets, which is realized by letting the label of data samples to conform to Dirichlet distribution. The extent of non-IID can be adjusted by tuning the concentration parameter ϕ of Dirichlet distribution.

Models: We adopt LeNet, Multilayer Perceptron (MLP), and VGG16 model. The introduction of these three models are as follows:

- LeNet: The LeNet model is one of the earliest published convolutional neural networks. For the experiments, like [39], we are going to train a LeNet model with two convolutional layers (both kernel size are 5 and the out channel of first one is 6 and second one is 16), two pooling layers (both kernel size are 2 and stride are 2), and three fully connected layer (the first one is (16×4) × 4, 120), the second is (120, 60) and the last is (60, 10)) for MNIST dataset. And for CIFAR10 dataset, we are going to train a LeNet model with two convolutional layers (both kernel size are 5 and the out channel are 64), two pooling layers (both kernel size are 2 and stride are 2), and three fully connected layer (the first one is (64×10^{-4}) 5×5 , 384), the second is (384, 192) and the last is (192, 10)). Cross-entropy function is taken as the training loss.
- MLP: The MLP model is a machine learning model based on Feedforward Neural Network that can achieve high-level feature extraction and classification. We configure the MLP model to be with three connected layers (the first one is $(28 \times 28, 200)$, the second is (200, 100)and the last is (100, 10)) like [40]. And for CIFAR10 dataset, we configure the MLP model to be with three connected layers (the first one is $(3 \times 32 \times 32, 200)$, the second is (200, 200) and the last is (200, 10)). And also cross-entropy function is taken as the training loss.

89.82

94.28

90.79

1,1011	,,,,,,,,,,,,,,,,,,,,,,,,,,,,,,,,,,,,,,,	annorone type	, ratios or	Djzum	1110 4114	ion, ama	Conce	Tir diron	param	cter on	1111 110 1	Guide	r una 1	301 (01 11	10001.	
	Attack Name		No Attack		Gaussia	n Attack			Sign-flip	Attack		LIE Attack				
Model	\bar{C}_{α}		0	0.1	0.2	0.3	0.4	0.1	0.2	0.3	0.4	0.1	0.2	0.3	0.4	
	ϕ	Algorithms		0.1	0.2	0.5	0.4	0.1	0.2	0.5	0.4	0.1	0.2	0.5	0.4	
		RAGA	97.89	97.78	97.79	97.82	97.75	97.72	97.76	97.69	97.25	97.79	97.82	97.80	97.71	
		FedAvg	95.54	10.28	11.35	11.35	11.35	94.03	9.80	9.82	9.80	95.10	94.96	93.66	92.63	
	0.6	Median	94.41	94.31	94.22	94.53	94.18	94.12	94.34	93.69	93.45	94.33	94.35	94.60	94.22	
	0.0	Byrd-SAGA	91.70	91.66	91.61	91.77	91.26	91.23	91.54	91.13	89.95	91.64	91.66	91.87	91.30	
		RFA	95.70	95.52	95.53	95.74	95.41	95.39	95.05	95.23	94.85	95.54	95.48	95.51	95.26	
LeNet		MCA	91.82	91.89	91.88	92.16	91.77	90.77	19.02	83.10	18.75	91.86	91.94	92.14	91.76	
Lenet		RAGA	97.62	97.47	97.67	97.50	97.30	97.42	97.16	97.28	97.38	97.75	97.64	97.60	97.28	
		FedAvg	95.13	9.80	11.35	10.32	9.80	10.10	10.10	10.09	9.80	94.81	94.38	93.74	92.09	
	0.2	Median	90.81	91.88	91.43	91.03	91.91	89.85	89.05	90.28	88.28	91.68	91.20	90.90	92.00	

89.77

94.61

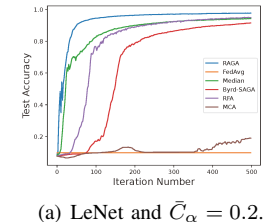
90.72

89.51

93.67

90.04

TABLE II: The maximum test accuracy(%) of 500 iteration number of RAGA, FedAvg, Median, Byrd-SAGA, RFA and MCA with different types, ratios of Byzantine attack, and concentration parameter on MNIST dataset and LeNet model.



Byrd-SAGA

RFA

MCA

90.36

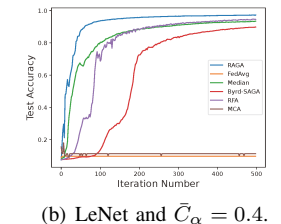
95.09

90.96

90.76

95.23

91.44



90.24

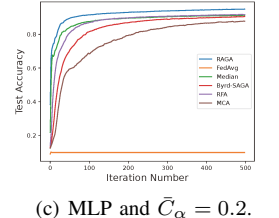
95.06

91.04

89.81

94.99

90.85



87.95

93.67

85.89

89.28

93.87

36.78

88.29

94.32

9.80

90.90

95.15

91.50

95.07

90.99

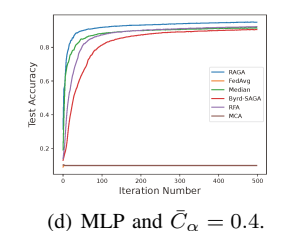


Fig. 2: Test accuracy of RAGA and baselines on $\phi = 0.6$, Sign-flip attack, and MNIST dataset.

• VGG16: The VGG16 model, originally developed by Simonyan and Zisserman from the Visual Geometry Group, represents a seminal 16-layer convolutional neural network architecture comprising 13 convolutional layers and 3 fully-connected (FC) layers. Each convolutional stage utilizes cascaded 3×3 kernels with stride 1 and ReLU activation, interspersed with 2×2 max-pooling operations that halve spatial resolution while preserving depth. The fully-connected hierarchy consists of two 4,096-unit hidden layers (FC1-2) followed by a 1,000-class output layer (FC3), totaling 138M trainable parameters. For CIFAR100 adaptation, we implemented fine-tuning to adapt to this dataset.

Byzantine attacks: The intensity level of Byzantine attack $\bar{C}_{\alpha} = 1 - C_{\alpha}$ is set to 0, 0.1, 0.2, 0.3, 0.4 and we select three types of Byzantine attack, which are introduced as follows:

- Gaussian attack: All Byzantine attacks are selected as the Gaussian attack, which obeys $\mathcal{N}(0, 90)$.
- Sign-flip attack: All Byzantine clients upload $-3 * \sum_{m \in \mathcal{M} \setminus \mathcal{B}} z_m^t$ to the central server on iteration number t.
- LIE attack [32]: LIE attack adds small amounts of noise to each dimension of the benign gradients. The noise is controlled by a coefficient c, which enables the attack to evade detection by robust aggregation methods while negatively impacting the global model. Specifically, the

attacker calculates the mean ρ and standard deviation ν of the parameters submitted by honest users, calculates the coefficient c based on the total number of honest and malicious clients, and finally computes the malicious update as $\rho + c\nu$. We set c to 0.7.

Hyperparameters: We assume M=50 and the batch-size of all the experiments is 32. The error tolerance ϵ for numerically working out geometric median and MCA are $\epsilon=1\times 10^{-5}$. The concentration parameter ϕ is set to 0.6, 0,4 and 0.2. The iteration number T=500 for both MNIST and CIFAR10 dataset, while T=100 for CIFAR100 dataset. In default, the round number of local updates $K^t=3$ for all algorithms on LeNet and MLP model, while $K^t=1$ on VGG16 model. In terms of the learning rate, we adopt default setup as shown in corresponding papers for baseline methods.

setup as shown in corresponding papers for baseline methods. For RAGA, the learning rate $\eta_m^{t,k}=\eta^t=\frac{K^t}{\sqrt{5}\sqrt{t+5}}=\frac{K^t}{5\sqrt{0.2t+1}}$ for LeNet and MLP models, while $\eta_m^{t,k}=\eta^t=\frac{4*10^{-2}K^t}{\sqrt{t+100}}=\frac{4*10^{-3}K^t}{\sqrt{0.01t+1}}$ for VGG16 model. This learning rate configuration is motivated by Remark 1, which is derived from Theorem 1 and tailored for non-convex loss functions, covering the experimental models including LeNet, MLP, and VGG16. It is worth noting that the learning rate used in

practice slightly deviates from that suggested in Remark 1 due

TABLE III: The maximum test accuracy(%) of 500 iteration number of RAGA, FedAvg, Median, Byrd-SAGA, RFA and MCA with different types, ratios of Byzantine attack, and concentration parameter on MNIST dataset and MLP model.

	Attack Name		No Attack		Gaussia	1 Attack			Sign-flip	Attack		LIE Attack				
Model		\bar{C}_{α}	0	0.1	0.2	0.3	0.4	0.1	0.2	0.3	0.4	0.1	0.2	0.3	0.4	
	ϕ	Algorithms		0.1	0.2	0.3		0.1	0.2	0.5	0.1	0.1	0.2	0.5	0.1	
		RAGA	95.23	95.10	95.06	95.01	94.98	94.84	95.00	94.23	95.01	95.08	95.16	95.02	94.92	
		FedAvg	92.09	23.10	24.69	25.17	9.84	89.41	10.10	9.80	10.32	91.92	90.44	87.98	85.85	
	0.6	Median	91.48	91.38	91.63	91.29	91.24	91.23	91.32	90.94	91.55	91.39	91.46	91.26	91.27	
MLP -	0.0	Byrd-SAGA	90.64	90.69	90.70	90.49	90.63	90.46	90.62	89.93	90.62	90.64	90.69	90.59	90.57	
		RFA	92.38	92.31	92.41	92.04	92.27	92.10	91.86	90.81	92.33	92.36	92.46	92.05	92.18	
		MCA	90.62	90.66	90.77	90.52	90.63	90.36	87.86	60.77	10.32	90.66	90.69	90.56	90.70	
MILF		RAGA	94.53	94.45	94.69	94.16	94.32	94.09	94.43	93.84	94.72	94.35	94.70	94.16	94.38	
		FedAvg	91.84	21.48	19.66	30.05	12.34	10.10	11.98	9.80	10.09	91.48	90.27	87.50	85.41	
	0.2	Median	89.54	89.16	89.74	89.04	89.37	88.65	89.70	87.14	89.83	89.22	89.70	89.18	89.51	
	0.2	Byrd-SAGA	90.24	90.12	90.08	89.96	89.76	89.86	90.08	88.40	90.06	90.04	90.08	89.92	89.85	
		RFA	92.01	91.88	91.92	91.65	91.66	91.72	91.91	91.23	92.04	91.89	91.95	91.62	91.49	
		MCA	90.32	90.21	90.40	90.23	89.99	89.63	81.01	94.81	10.28	90.29	90.32	90.21	89.91	
				1				•				•				
	- ea			15 — RAGA			0.45 (

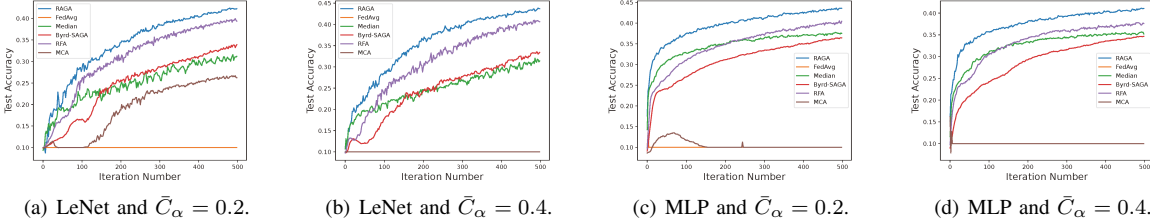


Fig. 3: Test accuracy of RAGA and baselines on $\phi = 0.6$, Sign-flip attack, and CIFAR10 dataset.

to implementation considerations. Specifically, we set $\delta=1/6$ and c=5 for LeNet and MLP, and $\delta=1/6$ and c=100 for VGG16. Since the exact smoothness constant L is unknown, we adopt heuristic coefficients, e.g., $\frac{K^t}{\sqrt{5}}$ for LeNet/MLP and $4*10^{-2}K^t$ for VGG16, to ensure the learning rate remains sufficiently small for convergence.

Baselines: The convergence performance of four algorithms: RAGA, FedAvg [16], Median [15], Byrd-SAGA [28], RFA [27], MCA [26] are compared. For the latter five algorithms, FedAvg is renowned in traditional FL but does not concern Byzantine attack and can be taken as a performance metric when there is no Byzantine attack, Median takes the coordinate-wise median of the uploaded vectors to update the global model parameter, Byrd-SAGA only executes one local updating in each round of iteration, RFA selects the trimmed mean of the model parameters over multiple local updating as the uploaded vector, and MCA utilizes its the maximum correntropy of the model parameters' distribution characteristics and compute the central value to update the global model parameter. It is worthy to note that there is another Byzantine-resilient FL algorithm in related works: BROADCAST [29]. We do not show the performance of it because BROADCAST is very similar with Byrd-SAGA and only differs from Byrd-SAGA by uploading vector from each user to the central server in a compressive, rather than lossless way like in Byrd-SAGA.

B. Convergence Performance

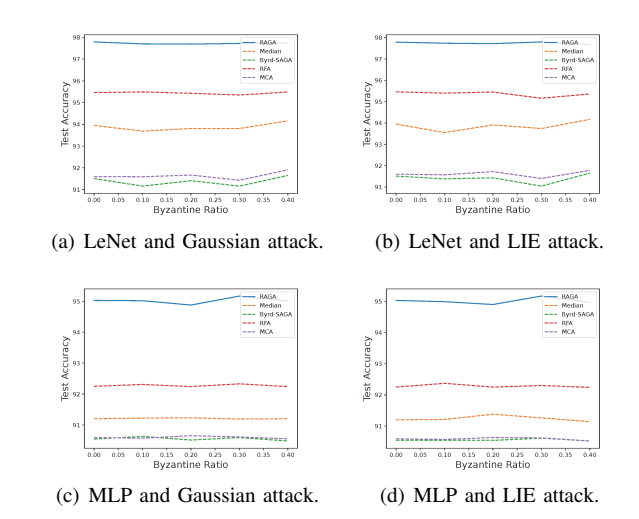


Fig. 4: The maximum test accuracy(%) of 500 iteration number of RAGA and baselines on $\phi = 0.4$ and MNIST dataset.

We begin with Table II, III, IV and V, which presents the maximum test accuracy of RAGA and baselines under varying

TABLE IV: The maximum test accuracy(%) of 500 iteration number of RAGA, FedAvg, Median, Byrd-SAGA, RFA and
MCA with different types, and ratios of Byzantine attack on CIFAR10 dataset and two learning models.

	Attack Name		No Attack		Gaussia	n Attack			Sign-flip	Attack		LIE Attack				
Model		\bar{C}_{lpha}	0	0.1	0.2	0.3	0.4	0.1	0.2	0.3	0.4	0.1	0.2	0.3	0.4	
	ϕ	Algorithms		0.1	0.2	0.5	0.4	0.1	0.2		0.4	0.1	0.2	0.5	0.4	
		RAGA	42.92	43.28	41.68	42.81	41.89	41.58	41.40	41.03	42.29	42.91	40.20	42.12	41.42	
LeNet		FedAvg	39.45	10.91	10.00	10.00	10.00	10.00	10.00	10.00	10.00	41.37	35.38	25.40	15.89	
	0.4	Median	32.17	31.70	30.83	31.59	30.29	30.09	30.54	28.00	30.19	31.50	30.83	32.25	31.25	
	0.4	Byrd-SAGA	34.81	34.60	33.86	33.92	34.27	33.49	33.66	29.37	34.21	35.20	34.19	33.89	34.64	
		RFA	41.85	41.64	41.65	41.42	41.27	40.92	41.61	37.20	41.65	41.78	41.32	41.21	40.88	
		MCA	35.10	34.83	34.26	34.23	34.69	32.92	18.01	10.00	10.00	34.42	34.21	34.64	34.53	
		RAGA	44.21	44.32	44.06	44.29	43.13	43.63	43.71	44.02	42.88	44.11	43.93	44.65	43.20	
		FedAvg	40.13	10.86	10.00	12.03	13.84	12.32	14.05	14.46	10.00	34.38	30.80	25.30	23.83	
MLP	0.4	Median	37.66	37.34	37.48	37.62	36.51	36.77	37.06	37.12	36.23	37.56	37.42	37.76	36.54	
WILI	0.4	Byrd-SAGA	37.38	36.72	36.93	36.85	36.01	36.34	37.03	36.52	35.99	36.78	37.03	36.89	36.18	
		RFA	40.53	40.41	40.26	40.94	39.85	37.91	40.28	39.61	40.08	40.69	40.51	40.72	39.97	
		MCA	37.18	36.87	36.94	36.99	36.36	36.47	14.68	15.40	10.00	36.63	37.18	37.00	35.97	

levels of Byzantine attack intensity \bar{C}_{α} , across different data heterogeneity concentration parameters ϕ , and for two learning models. Fig 2 and 3 illustrates the convergence of RAGA and the baselines under Sign-flip attack and data heterogeneity concentration parameters $\phi=0.6$. Fig 4, 5 and 6 present the maximum test accuracy of RAGA and the baseline methods under various Byzantine ratios, excluding the results reported in Table II, III and IV. Fig 7, 8 present the test accuracy of RAGA with different data heterogeneity parameters under various Byzantine ratios. And Fig 9 and 10 illustrates convergence of RAGA under different local epoch K on Gaussian attack with $\bar{C}_{\alpha}=0.2$. Following this, we will discuss the performance comparison between RAGA and the baselines in different scenarios.

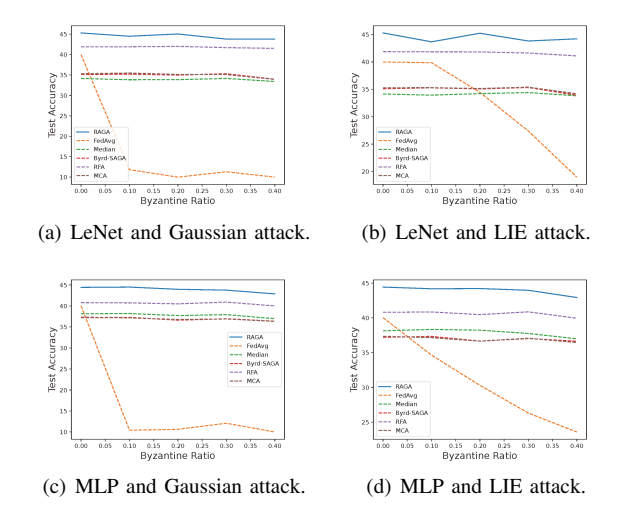


Fig. 5: The maximum test accuracy(%) of 500 iteration number of RAGA and baselines on $\phi=0.6$ and CIFAR10 dataset.

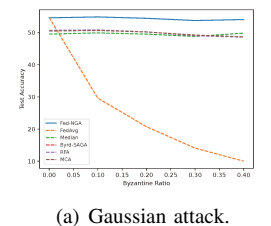
No Byzantine attack: For the easy dataset (MNIST), Table II, III and Fig. 4 show that RAGA outperforms all other

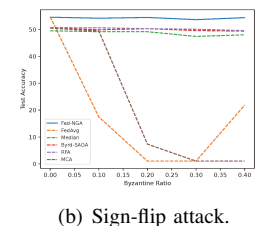
methods across a range of data heterogeneity concentration parameters, ϕ , and two different learning models. Specifically, compared to the baselines, RAGA increases test accuracy by 2.19% and 2.85% for the LeNet and MLP models, respectively, with $\phi = 0.6$, and by 2.49% and 2.52% for the LeNet and MLP models with $\phi = 0.2$. For the CIFAR10 dataset, Table IV and Fig. 5 demonstrate that RAGA also achieves the highest performance across different data heterogeneity concentrations, particularly for $\phi = 0.4$ with the LeNet and MLP models. In comparison to the baselines, RAGA increases test accuracy by 1.07% and 3.68% for the LeNet and MLP models, respectively, at $\phi = 0.4$, and consistently shows the highest accuracy at $\phi = 0.6$. As presented in Table V, when applied to the CIFAR100 dataset, RAGA demonstrates a notable improvement in test accuracy, achieving a 3.89% increase compared to the robust baselines. In contrast, the performance gap between RAGA and FedAvg is minimal, narrowing to just 0.1%.

Gaussian attack: First, we evaluate the performance of RAGA and the baseline methods on the MNIST dataset. As shown in Table II and III, RAGA achieves the highest test accuracy among all FL robust algorithms across different Byzantine attack ratios, two learning models, and two distinct data heterogeneity concentration parameters. For the LeNet model, RAGA shows an improvement in test accuracy by 2.08% to 2.34% for the data heterogeneity concentration parameter $\phi = 0.6$, and by 2.24% to 2.69% for $\phi = 0.2$, across four different Byzantine ratios ($\bar{C}_{\alpha} = 0.1, 0.2, 0.3, 0.4$). For the MLP model, RAGA improves test accuracy by 2.65% to 2.97% for $\phi = 0.6$, and by 2.57% to 2.77% for $\phi = 0.2$, across the same four Byzantine ratios. Additionally, as shown in Fig. 4, RAGA outperforms five other FL robust algorithms across various Byzantine attack ratios, regardless of the learning model type, when the data heterogeneity concentration parameter is set to $\phi = 0.4$. Next, we analyze the performance of RAGA and the baseline methods on the more complex CIFAR-10 dataset. With the data heterogeneity concentration parameter

TABLE V: The maximum test accuracy(%) of 100 iteration number of RAGA, FedAvg, Median, Byrd-SAGA, RFA and MCA with different types, and ratios of Byzantine attack on CIFAR100 dataset and VGG16 model.

	Attack Name		No Attack		Gaussia	n Attack			Sign-flip	Attack		LIE Attack				
Model		\bar{C}_{α}	0	0.1	0.2	0.3	0.4	0.1	0.2	0.3	0.4	0.1	0.2	0.3	0.4	
	ϕ	Algorithms		0.1	0.2	0.3	0.1	0.1		0.5	0.4	0.1	0.2	0.5	0.4	
		RAGA	54.57	54.85	54.42	53.73	54.03	54.19	54.48	53.66	54.40	54.61	54.55	54.62	53.71	
		FedAvg	54.67	29.59	20.73	14.06	10.02	17.45	1.00	1.00	21.88	53.38	52.03	50.71	49.86	
VGG16	0.6	Median	49.51	49.89	49.50	48.79	49.81	49.17	49.15	47.42	48.01	49.39	48.97	48.80	48.75	
70010	0.0	SAGA	50.50	50.78	50.19	49.11	48.64	49.88	50.30	49.60	49.38	50.47	50.05	49.66	48.91	
		RFA	50.68	50.80	50.22	49.01	48.57	50.62	50.29	50.09	49.55	50.42	50.04	49.73	48.92	
		MCA	50.48	50.64	50.17	49.21	48.66	49.41	7.32	1.00	1.00	50.43	50.00	49.63	48.88	





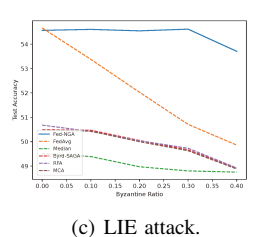


Fig. 6: The maximum test accuracy (%) of 100 iteration number of RAGA and baselines on $\phi = 0.6$ and CIFAR100 dataset.

 $\phi=0.4$, RAGA consistently outperforms all baseline methods in terms of test accuracy, as shown in Table IV. Specifically, for the LeNet model, RAGA achieves improvements by 0.03% to 1.64%, while for the MLP model, improvements by 3.25% to 3.91%, across four different Byzantine ratios ($\bar{C}_{\alpha}=0.1,0.2,0.3,0.4$). Furthermore, RAGA consistently performs better than all baseline methods based on Fig. 5, irrespective of whether the LeNet or MLP model is used, when the data heterogeneity concentration parameter is set to $\phi=0.6$. For the CIFAR100 dataset, Table V demonstrates that RAGA achieves a maximum accuracy improvement of 4.05% to 4.52% across four distinct Byzantine ratios when compared to baseline methods. Additionally, as shown in Fig. 6, RAGA consistently outperforms all baselines on the VGG16 model under Gaussian attacks.

Sign-flip attack: First, for the relatively simple dataset (MNIST), as shown in Table II and III, all FL robust methods, with the exception of MCA, effectively mitigate the sign-flip attack across various Byzantine ratios. In contrast, MCA fails to defend against this attack at higher Byzantine ratios. For the LeNet model, Table II and III show that RAGA outperforms all other methods in terms of test accuracy, improving by 2.33% to 2.71% with the data heterogeneity concentration parameter of $\phi = 0.6$, and by 3.06% to 3.75% with $\phi = 0.2$, across four different Byzantine ratios. For the MLP model, RAGA also achieves the highest test accuracy among all baseline methods, improving by 2.68% to 3.42% for $\phi = 0.6$, and by -0.97% to 2.68% for $\phi = 0.2$, across the same four Byzantine ratios. Then, for the more complex dataset (CIFAR10), as shown in Table IV, similar to the results on the MNIST dataset, all FL robust methods, except MCA, effectively mitigate the sign-flip attack across various Byzantine ratios. With the data heterogeneity concentration parameter of $\phi = 0.4$, RAGA

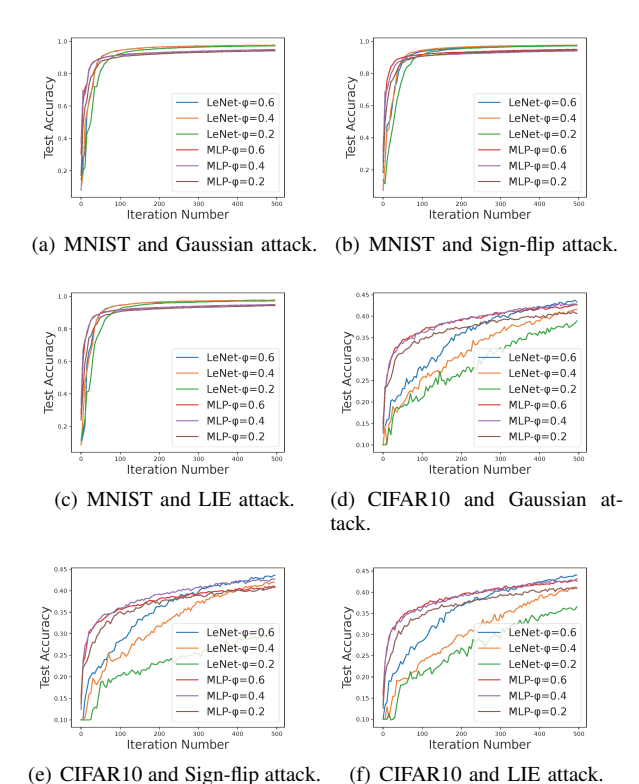


Fig. 7: Test accuracy of RAGA with different data heterogeneity parameters on $\bar{C}_{\alpha}=0.4$.

performs the best in most cases (except for the LeNet model with $\bar{C}_{\alpha}=0.2$), with test accuracy improvements of -0.21% to 4.01% for the LeNet model, and 2.8% to 5.72% for the MLP model, across the four Byzantine ratios. Additionally, as shown

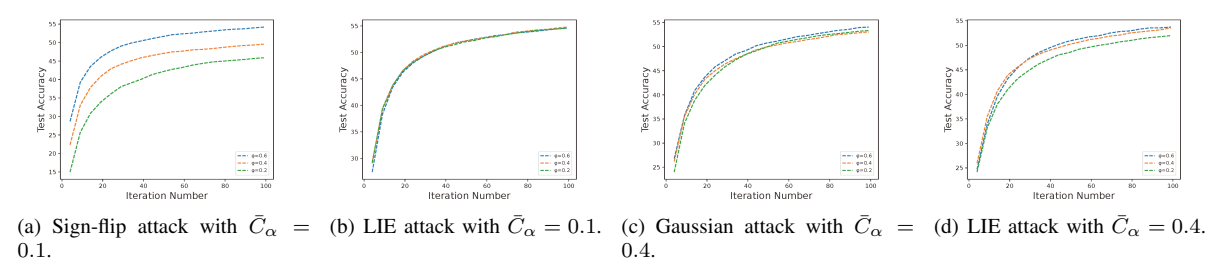


Fig. 8: Test accuracy of RAGA with different data heterogeneity parameters on CIFAR100 dataset.

in Fig. 2 and 3, RAGA achieves the fastest convergence speed among all baseline methods with the same local epoch $K^t=3$ and data heterogeneity concentration parameter $\phi=0.6$, regardless of the learning model type or the Byzantine ratio. According to Table V, for the CIFAR100 dataset, RAGA consistently boosts test accuracy by 3.57% to 4.85% across four distinct Byzantine ratios compared to baselines when $\phi=0.6$. Fig. 6 further illustrates that RAGA outperforms all baselines across the evaluated conditions. Regarding the FedAvg result with $C_{\alpha}=0.4$ that exhibits a seemingly "maximum" accuracy, this outcome should not be attributed to statistical abnormality. Instead, the extremely high loss value of 856667.4125 indicates that the model likely converged to a distant saddle point in the loss landscape.

LIE attack: Using the simple MNIST dataset, RAGA achieves the best performance among six baseline methods across four Byzantine ratios. As shown in Table II and III, for the LeNet model, RAGA improves test accuracy by 2.25% to 2.45% when the data heterogeneity concentration parameter is $\phi = 0.6$, and by 2.57% to 3.00% when $\phi = 0.2$, across four different Byzantine ratios. Similarly, for the MLP model, RAGA outperforms all baseline methods, improving test accuracy by 2.7% to 2.97% when the data heterogeneity concentration parameter is $\phi = 0.6$, and by 2.46% to 2.89% when $\phi = 0.2$. Furthermore, as shown in Fig. 4, with a data heterogeneity concentration parameter of $\phi = 0.4$, RAGA achieves the best test accuracy performance among five FL Byzantine-robust algorithms, regardless of the type of learning model. Additionally, using the more complex CIFAR-10 dataset, RAGA outperforms most baseline methods (with the exception of the LeNet model at a Byzantine ratio of $C_{\alpha} = 0.2$). With the data heterogeneity concentration parameter of $\phi = 0.4$, RAGA enhances test accuracy by -1.12% to 1.13% on the LeNet model, and by 3.23% to 3.93% on the MLP model, across four Byzantine ratios, compared to other FL Byzantine-robust algorithms. Finally, as shown in Fig. 5, under the LIE attack, RAGA also outperforms all six baseline methods with the data heterogeneity concentration parameter $\phi = 0.6$. Regarding the CIFAR100 dataset, RAGA demonstrates superior performance against LIE attacks, achieving improvements in test accuracy ranging from 1.23% to 3.91% across four distinct Byzantine ratios when compared to baseline methods, as shown in Table V. Additionally, Fig. 6 confirms that RAGA establishes state-of-the-art (SoTA) performance under these experimental settings, outperforming all baseline approaches evaluated.

Data Heterogeity: We first analyze the convergence performance of RAGA on the MNIST dataset. As shown in Table II and III, varying data heterogeneity parameters has minimal impact on the test accuracy of RAGA, with the maximum difference being only 0.66%, as further confirmed by Fig. 7. In contrast, for the more complex CIFAR10 dataset, the effect of different data heterogeneity parameters on RAGA's test accuracy is more pronounced, as depicted in Fig. 7. Additionally, we observe that the MLP model is more robust to data heterogeneity than the LeNet model, particularly in the presence of the Sign-flip attack. For the CIFAR100 dataset, as depicted in Fig. 8, the experimental results on the VGG16 model demonstrate that the impact of attack type on accuracy surpasses that of data heterogeneity. This distinction is notably evident when comparing the Sign-flip and LIE attacks, where differing attack strategies produce more significant effects on model accuracy than variations in data distribution heterogeneity.

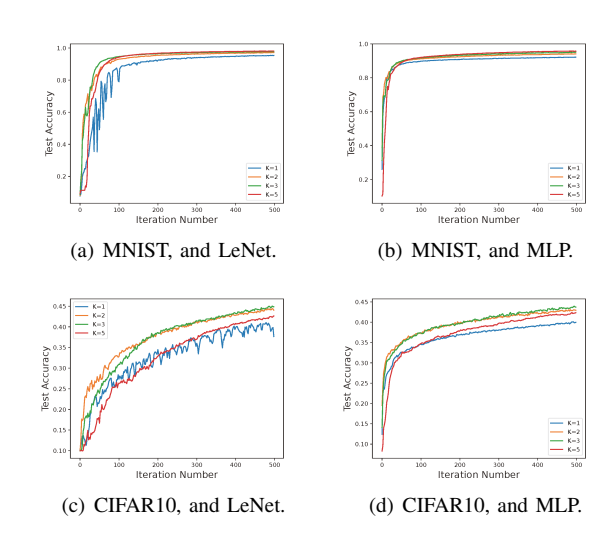


Fig. 9: Test accuracy of RAGA with different local epoch on Gaussian attack on $\bar{C}_{\alpha}=0.2$ with $\phi=0.6$.

Local update: From Fig. 9 and 10, it is clear that a larger local update size K does not necessarily result in better performance, which is consistent with our theoretical analysis, irrespective of the learning model or dataset. With the LeNet model, the convergence curve exhibits significant fluctuations when K=1, leading to suboptimal convergence performance. When K=5, although the fluctuations are

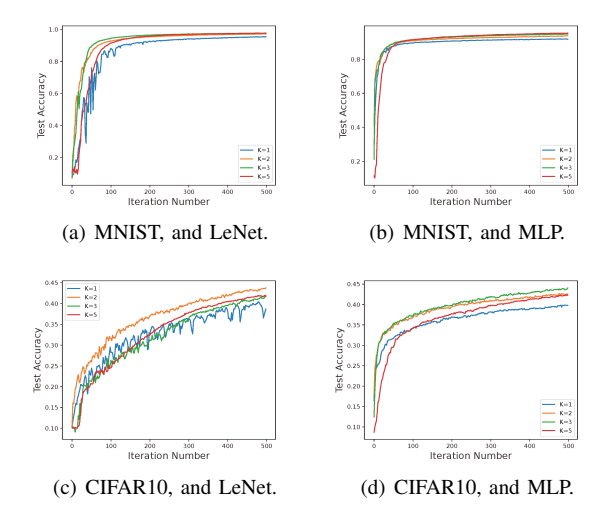


Fig. 10: Test accuracy of RAGA with different local epoch on Gaussian attack on $\bar{C}_{\alpha} = 0.2$ with $\phi = 0.2$.

reduced, the increased number of training rounds adversely affects the algorithm's performance. In contrast, for K=2 or K=3, the choice of K demonstrates distinct advantages across both datasets and learning models. These experimental findings are in agreement with our theoretical proof.

In summary, the above numerical experiments demonstrate that RAGA not only outperforms its competitors across different ratios and types of Byzantine attacks but also performs comparably to FedAvg, which excels when there is no Byzantine attack. It is also noteworthy that the RAGA algorithm can converge under various types of Byzantine attacks. Lastly, all these results are based on non-IID datasets with three different data heterogeneity concentration parameters.

VI. CONCLUSION

In this paper, we propose a novel FL aggregation strategy, RAGA, designed to be robust against Byzantine attacks and data heterogeneity. Our proposed RAGA leverages the geometric median for aggregation, allowing flexible selection of the round number for local updates. Rigorous proofs reveal that RAGA can achieve a convergence rate of $\mathcal{O}(1/T^{2/3-\delta})$ for non-convex loss functions, with $\delta \in (0,2/3)$, and a linear rate for strongly-convex loss functions, provided that the fraction of the dataset from malicious users is less than half. Experimental results on heterogeneous datasets demonstrate that RAGA consistently outperforms baseline methods in convergence performance under varying intensities of Byzantine attacks.

REFERENCES

- L. Zhou, K.-H. Yeh, G. Hancke, Z. Liu, and C. Su, "Security and privacy for the industrial internet of things: An overview of approaches to safeguarding endpoints," *IEEE Signal Process. Mag.*, vol. 35, no. 5, pp. 76–87, 2018.
- [2] H. B. McMahan, F. Yu, P. Richtarik, A. Suresh, and D. Bacon, "Federated learning: Strategies for improving communication efficiency," *Proc. Adv. Conf. Neural Inf. Process. Syst.*, pp. 5–10, 2016.
- [3] T. Li, A. K. Sahu, M. Zaheer, M. Sanjabi, A. Talwalkar, and V. Smith, "Federated optimization in heterogeneous networks," *Proc. Mach. Learn. Syst.*, pp. 429–450, 2020.

- [4] R. Agrawal and R. Srikant, "Privacy-preserving data mining," Proc. Int. Conf. Manage. Data, pp. 439–450, 2000.
- [5] J. Duchi, M. J. Wainwright, and M. I. Jordan, "Local privacy and minimax bounds: Sharp rates for probability estimation," *Proc. Int. Conf. Neural Inf. Process. Syst.*, pp. 1529–1537, 2013.
- [6] J. Konečný, H. B. McMahan, D. Ramage, and P. Richtárik, "Federated optimization: Distributed machine learning for on-device intelligence," arXiv preprint arXiv:1610.02527, 2016.
- [7] S. Wang, T. Tuor, T. Salonidis, K. K. Leung, C. Makaya, T. He, and K. Chan, "Adaptive federated learning in resource constrained edge computing systems," *IEEE J. Sel. Areas Commun.*, vol. 37, no. 6, pp. 1205–1221, 2019.
- [8] M. Chen, D. Gündüz, K. Huang, W. Saad, M. Bennis, A. V. Feljan, and H. V. Poor, "Distributed learning in wireless networks: Recent progress and future challenges," *IEEE J. Sel. Areas Commun.*, vol. 39, no. 12, pp. 3579–3605, 2021.
- [9] A. Vempaty, L. Tong, and P. K. Varshney, "Distributed inference with byzantine data: State-of-the-art review on data falsification attacks," *IEEE Signal Process. Mag.*, vol. 30, no. 5, pp. 65–75, 2013.
- [10] Z. Yang, A. Gang, and W. U. Bajwa, "Adversary-resilient distributed and decentralized statistical inference and machine learning: An overview of recent advances under the byzantine threat model," *IEEE Signal Process. Mag.*, vol. 37, no. 3, pp. 146–159, 2020.
- [11] J. So, B. Güler, and A. S. Avestimehr, "Byzantine-resilient secure federated learning," *IEEE J. Sel. Areas Commun.*, vol. 39, no. 7, pp. 2168–2181, 2020.
- [12] X. Cao and L. Lai, "Distributed gradient descent algorithm robust to an arbitrary number of byzantine attackers," *IEEE Trans. Signal Process.*, vol. 67, no. 22, pp. 5850–5864, 2019.
- [13] Y. Chen, L. Su, and J. Xu, "Distributed statistical machine learning in adversarial settings: Byzantine gradient descent," *Proc. ACM Meas. Anal. Comput. Syst.*, pp. 1–25, 2017.
- [14] X. Cao and L. Lai, "Distributed approximate newton's method robust to byzantine attackers," *IEEE Trans. Signal Process.*, vol. 68, pp. 6011– 6025, 2020.
- [15] C. Xie, O. Koyejo, and I. Gupta, "Generalized byzantine-tolerant SGD," arXiv preprint arXiv:1802.10116, 2018.
- [16] Y. Zhao, M. Li, L. Lai, N. Suda, D. Civin, and V. Chandra, "Federated learning with non-iid data," arXiv preprint arXiv:1806.00582, 2018.
- [17] Z. Xie and S. Song, "FedKL: Tackling data heterogeneity in federated reinforcement learning by penalizing kl divergence," *IEEE J. Sel. Areas Commun.*, vol. 41, no. 4, pp. 1227–1242, 2023.
- [18] D. Yin, Y. Chen, R. Kannan, and P. Bartlett, "Byzantine-robust distributed learning: Towards optimal statistical rates," *Proc. Int. Conf. Machine Learning*, pp. 5650–5659, 2018.
- [19] B. Turan, C. A. Uribe, H.-T. Wai, and M. Alizadeh, "Robust distributed optimization with randomly corrupted gradients," *IEEE Trans. Signal Process.*, vol. 70, pp. 3484–3498, 2022.
- [20] P. Zhao, F. Yu, and Z. Wan, "A huber loss minimization approach to byzantine robust federated learning," *AAAI Conf. Artif. Intell.*, vol. 38, no. 19, pp. 21 806–21 814, 2024.
- [21] L. Su and J. Xu, "Securing distributed gradient descent in high dimensional statistical learning," *Proc. ACM Meas. Anal. Comput. Syst.*, no. 1, pp. 1–41, 2019.
- [22] P. Zhao and Z. Wan, "High dimensional distributed gradient descent with arbitrary number of byzantine attackers," arXiv preprint arXiv:2307.13352, 2023.
- [23] P. Blanchard, E. M. El Mhamdi, R. Guerraoui, and J. Stainer, "Machine learning with adversaries: Byzantine tolerant gradient descent," *Proc.* 31st Int. Conf. Neural Inf. Process. Syst., pp. 118–128, 2017.
- [24] X. Fan, Y. Wang, Y. Huo, and Z. Tian, "BEV-SGD: Best effort voting SGD against byzantine attacks for analog-aggregation-based federated learning over the air," *IEEE Internet Things J.*, vol. 9, no. 19, pp. 18946– 18959, 2022.
- [25] L. Li, W. Xu, T. Chen, G. B. Giannakis, and Q. Ling, "RSA: Byzantine-robust stochastic aggregation methods for distributed learning from heterogeneous datasets," *Proc. AAAI Conf. Artif. Intell.*, no. 01, pp. 1544–1551, 2019.
- [26] Z. Luan, W. Li, M. Liu, and B. Chen, "Robust federated learning: Maximum correntropy aggregation against byzantine attacks," *IEEE Trans. Neural Networks Learn. Syst.*, 2024.
- [27] K. Pillutla, S. M. Kakade, and Z. Harchaoui, "Robust aggregation for federated learning," *IEEE Trans. Signal Process.*, vol. 70, pp. 1142– 1154, 2022.
- [28] Z. Wu, Q. Ling, T. Chen, and G. B. Giannakis, "Federated variancereduced stochastic gradient descent with robustness to byzantine attacks," *IEEE Trans. Signal Process.*, vol. 68, pp. 4583–4596, 2020.

- [29] H. Zhu and Q. Ling, "Byzantine-robust distributed learning with compression," *IEEE Trans. Signal Inf. Process. Netw.*, vol. 9, pp. 280 – 294, 2023.
- [30] W. Huang, Z. Shi, M. Ye, H. Li, and B. Du, "Self-driven entropy aggregation for byzantine-robust heterogeneous federated learning," in Int. Conf. Artif. Intell. Stats. PMLR, 2024.
- [31] D. Data and S. Diggavi, "Byzantine-resilient high-dimensional sgd with local iterations on heterogeneous data," in *Int. Conf. Artif. Intell. Stats*. PMLR, 2021, pp. 2478–2488.
- [32] G. Baruch, M. Baruch, and Y. Goldberg, "A little is enough: Circumventing defenses for distributed learning," *Proc. Adv. Neural Inf. Process. Syst.*, vol. 32, 2019.
- [33] C. Xie, O. Koyejo, and I. Gupta, "Fall of empires: Breaking byzantinetolerant sgd by inner product manipulation," pp. 261–270, 2020.
- [34] S. Minsker, "Geometric median and robust estimation in banach spaces," *Bernoulli*, pp. 2308–2335, 2015.
- [35] A. Defazio, F. Bach, and S. Lacoste-Julien, "SAGA: A fast incremental gradient method with support for non-strongly convex composite objectives," *Proc. Adv. Neural Inf. Process. Syst.*, pp. 1646–1654, 2014.
- [36] K. Aftab, R. Hartley, and J. Trumpf, "Generalized weiszfeld algorithms for lq optimization," *IEEE Trans. Pattern Anal. Mach. Intell.*, vol. 37, no. 4, pp. 728–745, 2014.
- [37] M. Huang, D. Zhang, and K. Ji, "Achieving linear speedup in non-iid federated bilevel learning," *arXiv preprint arXiv:2302.05412*, 2023.
- [38] X. Li and P. Li, "Analysis of error feedback in federated non-convex optimization with biased compression," arXiv preprint arXiv:2211.14292, 2022.
- [39] Y. LeCun, L. Bottou, Y. Bengio, and P. Haffner, "Gradient-based learning applied to document recognition," *Proc. IEEE*, vol. 86, no. 11, pp. 2278– 2324, 1998.
- [40] K. Yue, R. Jin, R. Pilgrim, C.-W. Wong, D. Baron, and H. Dai, "Neural tangent kernel empowered federated learning," *Proc. Int. Conf. Mach. Learn.*, pp. 25783–25803, 2022.



Rongfei Fan (Member, IEEE) received the B.E. degree in communication engineering from Harbin Institute of Technology, Harbin, China, in 2007, and the Ph. D degree in electrical engineering from the University of Alberta, Edmonton, Alberta, Canada, in 2012. Since 2013, he has been a faculty member at the Beijing Institute of Technology, Beijing, China, where he is currently an Associate Professor in the School of Cyberspace Science and Technology. His research interests include federated learning, semantic communications, edge computing, and resource

allocation in wireless networks.



Han Hu (Member, IEEE) is currently a Professor with the School of Information and Electronics, Beijing Institute of Technology, China. He received the B.E. and Ph.D. degrees from the University of Science and Technology of China, China, in 2007 and 2012 respectively. His research interests include multimedia networking, edge intelligence and spaceair-ground integrated network. He received several academic awards, including Best Paper Award of IEEE TCSVT 2019, Best Paper Award of IEEE Multimedia Magazine 2015, Best Paper Award of

IEEE Globecom 2013, etc. He served as an Associate Editor of IEEE TMM and Ad Hoc Networks, and a TPC Member of Infocom, ACM MM, AAAI, IJCAI, etc.



Shiyuan Zuo received the B.E. degree from the Beijing Institute of Technology, China, in 2021. He is currently pursuing a Ph.D. degree at the School of Cyberspace Science and Technology, Beijing Institute of Technology, China. His research interests include federated learning and privacy protection.



Hangguan Shan (Senior Member, IEEE) received the B.Sc. degree in electrical engineering from Zhejiang University, Hangzhou, China, in 2004, and the Ph.D. degree in electrical engineering from Fudan University, Shanghai, China, in 2009. From 2009 to 2010, he was a Postdoctoral Research Fellow with the University of Waterloo, Waterloo, ON, Canada. Since 2011, he has been with the College of Information Science and Electronic Engineering, Zhejiang University, where he is currently an Associate Professor. He is also with the Zhejiang Provincial

Key Laboratory of Information Processing and Communication Networks, Zhejiang University. His current research interests include machine learningenabled resource allocation and quality-of-service provisioning in wireless networks. Dr. Shan has co-received the Best Industry Paper Award from the IEEE WCNC'11 and the Best Paper Award from the IEEE WCSP'23. He has served as a Technical Program Committee Member of various international conferences. He was an Editor of the IEEE TRANSACTIONS ON GREEN COMMUNICATIONS AND NETWORKING.



Xingrun Yan received the B.E. degree from Beijing Institute of Technology, China, in 2022. He is currently pursuing the master's degree with the School of Cyberspace Science and Technology, Beijing Institute of Technology, China. His research interests include federated learning and semantic communications.



Tony Q. S. Quek (Fellow, IEEE) received the B.E. and M.E. degrees in electrical and electronics engineering from the Tokyo Institute of Technology in 1998 and 2000, respectively, and the Ph.D. degree in electrical engineering and computer science from the Massachusetts Institute of Technology in 2008. Currently, he is the Cheng Tsang Man Chair Professor with Singapore University of Technology and Design (SUTD) and ST Engineering Distinguished Professor. He also serves as the Director of the Future Communications R & D Programme, the

Head of ISTD Pillar, and the Deputy Director of the SUTDZJU IDEA. His current research topics include wireless communications and networking, network intelligence, non-terrestrial networks, open radio access network, and 6G

Dr. Quek has been actively involved in organizing and chairing sessions, and has served as a member of the Technical Program Committee as well as symposium chairs in a number of international conferences. He is currently serving as an Area Editor for the IEEE TRANSACTIONS ON WIRELESS COMMUNICATIONS.

Dr. Quek was honored with the 2008 Philip Yeo Prize for Outstanding Achievement in Research, the 2012 IEEE William R. Bennett Prize, the 2015 SUTD Outstanding Education Awards – Excellence in Research, the 2016 IEEE Signal Processing Society Young Author Best Paper Award, the 2017 CTTC Early Achievement Award, the 2017 IEEE ComSoc AP Outstanding Paper Award, the 2020 IEEE Communications Society Young Author Best Paper Award, the 2020 IEEE Stephen O. Rice Prize, the 2020 Nokia Visiting Professor, and the 2022 IEEE Signal Processing Society Best Paper Award. He is the AI on RAN Working Group Chair in AI-RAN Alliance. He is a Fellow of IEEE, a Fellow of WWRF, and a Fellow of the Academy of Engineering Singapore.



Puning Zhao received the B.S. degree from the University of Science and Technology of China, Hefei, China, in 2017, and the Ph.D. degree from the University of California at Davis, Davis, CA, USA, in 2021. He is currently an associate professor at School of Cyber Science and Technology, Shenzhen Campus of Sun Yat-sen University.

APPENDIX A

ASSUMPTIONS AND THEORETICAL RESULTS

In this section, we provide assumptions and theoretical results of the RAGA under Byzantine attacks. Below, we first present the necessary assumptions.

A. Assumption

For all honest users $m \in \mathcal{M} \setminus \mathcal{B}$, we have the following assumptions.

Assumption 7 (Lipschitz Continuity): The loss function f(w, s) has L-Lipschitz continuity [37], [38], i.e., for $\forall w_1, w_2 \in \mathbb{R}^p$, there is

$$f(\boldsymbol{w}_{1}, \boldsymbol{s}) - f(\boldsymbol{w}_{2}, \boldsymbol{s}) \leqslant \langle \nabla f(\boldsymbol{w}_{2}, \boldsymbol{s}), \boldsymbol{w}_{1} - \boldsymbol{w}_{2} \rangle + \frac{L}{2} \|\boldsymbol{w}_{1} - \boldsymbol{w}_{2}\|^{2}, \quad (30)$$

which is equivalent to the following inequality,

$$\|\nabla f(\boldsymbol{w}_1, \boldsymbol{s}) - \nabla f(\boldsymbol{w}_2, \boldsymbol{s})\| \leqslant L \|\boldsymbol{w}_1 - \boldsymbol{w}_2\|. \tag{31}$$

With (30) or (31), it can be derived that the global loss function F(w) and local loss function $F_m(w)$ both have L-Lipschitz continuity.

Assumption 8 (Strongly-Convex): The loss function $f(\boldsymbol{w}, \boldsymbol{s})$ is μ strongly-convex [37], i.e., for $\forall \boldsymbol{w}_1, \boldsymbol{w}_2 \in \mathbb{R}^p$, there is

$$\|\nabla f(\mathbf{w}_1, \mathbf{s}) - \nabla f(\mathbf{w}_2, \mathbf{s})\| \ge \mu \|\mathbf{w}_1 - \mathbf{w}_2\|.$$
 (32)

Similarly, with (32), F(w) and $F_m(w)$ can be derived to be both μ strongly-convex.

Assumption 9 (Local Unbiased Gradient): Suppose a subset of dataset S_m is selected randomly, which is denote as ξ_m , define

$$F_m(\boldsymbol{w}; \xi_m) \triangleq \frac{1}{|\xi_m|} \sum_{\boldsymbol{s} \in \mathcal{E}_m} f(\boldsymbol{w}, \boldsymbol{s}),$$
 (33)

the unbiased gradient [37], [38] implies that

$$\mathbb{E}\left\{\nabla F_m(\boldsymbol{w}; \boldsymbol{\xi}_m)\right\} = \nabla F_m(\boldsymbol{w}). \tag{34}$$

Assumption 10 (Bounded Inner Variance): For each honest user m and $\mathbf{w} \in \mathbb{R}^p$, the variance of stochastic local gradient $\nabla F_m(\mathbf{w}; \xi_m)$ is upper-bounded [37], [38] by

$$Var(\nabla F_m(\boldsymbol{w}; \xi_m)) \leqslant \sigma^2. \tag{35}$$

Assumption 11 (Data Heterogeneity): For each honest user m and $w \in \mathbb{R}^p$, the data heterogeneity can be defined as

$$\theta_m = \|\nabla F_m(\boldsymbol{w}) - \nabla F(\boldsymbol{w})\|. \tag{36}$$

We also assume the data heterogeneity is bounded [37], [38], which implies

$$\theta_m \leqslant \theta.$$
 (37)

Assumption 12 (Bounded Gradient): For each honest user m and $\mathbf{w} \in \mathbb{R}^p$, the ideal local gradient $\nabla F_m(\mathbf{w})$ is upperbounded [37], [38] by

$$\|\nabla F_m(\boldsymbol{w})\| \leqslant G. \tag{38}$$

B. Theoretical Results

In this subsection, we present the analytical results of convergence on our proposed RAGA. All proofs are deferred to Appendices B and C.

1) Case I: With Lipschitz Continuity Only for Loss Function: We first inspect the case with Assumptions 7, 9, 10, 11 and 12 imposed, which allows the loss function to be nonconvex. By defining

$$\alpha_m = \frac{S_m}{\sum_{j=1}^M S_j}, C_\alpha = \sum_{m \in \mathcal{M} \setminus \mathcal{B}} \alpha_m, \tag{39}$$

and

$$p^{t} = \begin{cases} 0, & \eta^{t} \leqslant \frac{1}{L} \\ 1, & \eta^{t} > \frac{1}{L} \end{cases}$$

$$\tag{40}$$

the following results can be expected.

Theorem 3: With $C_{\alpha} > 0.5$, there is

$$\sum_{t=1}^{T} \frac{\eta^{t}}{\sum_{t'=1}^{T} \eta^{t'}} \mathbb{E} \left\{ \left\| \nabla F(\boldsymbol{w}^{t}) \right\|^{2} \right\}
\leq \frac{2\mathbb{E} \left\{ F(\boldsymbol{w}^{1}) - F(\boldsymbol{w}^{T}) \right\}}{\sum_{t'=1}^{T} \eta^{t'}} + \frac{1}{\sum_{t'=1}^{T} \eta^{t'}} \sum_{t=1}^{T} \eta^{t} \Delta^{t}
+ \sum_{t=1}^{T} \frac{2(\eta^{t} + p^{t}(\eta^{t})^{2}L - p^{t}\eta^{t})\epsilon^{2}}{(2C_{\alpha} - 1)^{2} \sum_{t'=1}^{T} \eta^{t'}}
+ \sum_{t=1}^{T} \frac{8(C_{\alpha})^{2}(\eta^{t}\sigma^{2} + (p^{t}(\eta^{t})^{2}L - p^{t}\eta^{t})(G^{2} + \sigma^{2}))}{(2C_{\alpha} - 1)^{2} \sum_{t'=1}^{T} \eta^{t'}}, \tag{41}$$

where

$$\Delta^{t} = \frac{8C_{\alpha}}{(2C_{\alpha} - 1)^{2}} \sum_{m \in \mathcal{M} \setminus \mathcal{B}} \left(\frac{2\alpha_{m}L^{2}(G^{2} + \sigma^{2})}{K^{t}} \sum_{k=2}^{K^{t}} (k - 1) \cdot \sum_{i=1}^{k-1} (\eta_{m}^{t,i})^{2} + 2\alpha_{m}\theta^{2} \right).$$
(42)

Proof: Please refer to Appendix B.

2) Case II: With Lipschitz Continuity and Strong Convexity for Loss Function: For the case with Assumptions 7, 8, 9, 10, 11 and 12 imposed, which requires the loss function to be not only Lipschitz but also strongly-convex, the following results can be anticipated.

Theorem 4: With $0 < \lambda^t < 1$ and $C_{\alpha} > 0.5$, the optimality gap $\mathbb{E}\left\{F(\boldsymbol{w}^T) - F(\boldsymbol{w}^*)\right\}$ is upper bounded in (43) as follows,

$$\mathbb{E}\left\{F(\boldsymbol{w}^{T}) - F(\boldsymbol{w}^{*})\right\}$$

$$\leq \frac{L}{2}\mathbb{E}\left\{\left\|\boldsymbol{w}^{1} - \boldsymbol{w}^{*}\right\|^{2}\right\} \prod_{t=1}^{T-1} \gamma^{t} + \frac{L}{2} \sum_{t=1}^{T-1} \frac{(\eta^{t})^{2}}{\lambda^{t}} \left(\Delta^{t} + \frac{8\sigma^{2}(C_{\alpha})^{2}}{(2C_{\alpha} - 1)^{2}} + \frac{2\epsilon^{2}}{(2C_{\alpha} - 1)^{2}}\right) \cdot \prod_{i=t}^{T-1} (\gamma^{i+1})^{q^{i+1}},$$

$$(43)$$

where

$$q^t = \begin{cases} 0, & t = T \\ 1, & t < T \end{cases},$$

and

$$\gamma^{t} = \frac{1 - 2\eta^{t}\mu + L^{2}(\eta^{t})^{2}}{1 - \lambda^{t}}.$$

Proof: Please refer to Appendix C.

APPENDIX B PROOF OF THEOREM 3

The proof of Theorem 3 relies on the holding of Lemma 1 and Lemma 2, which is given as follows:

Lemma 1: With Assumptions 7, 9, 10, 11, 12, and $C_{\alpha} > 0.5$, the term $\mathbb{E}\left\{\left\|\boldsymbol{z}^{t} - \nabla F(\boldsymbol{w}^{t})\right\|^{2}\right\}$ can be upper bounded as

$$\mathbb{E}\left\{\left\|\boldsymbol{z}^{t} - \nabla F(\boldsymbol{w}^{t})\right\|^{2}\right\} \leqslant \Delta^{t} + \frac{8\sigma^{2}(C_{\alpha})^{2}}{(2C_{\alpha} - 1)^{2}} + \frac{2\epsilon^{2}}{(2C_{\alpha} - 1)^{2}}.$$
(44)

Proof: Please refer to Appendix D.

Lemma 2: With Assumptions 9, 10, 12, and $C_{\alpha} > 0.5$, the term $\mathbb{E}\left\{\left\|\boldsymbol{z}^{t}\right\|^{2}\right\}$ can be bounded as

$$0 \leqslant \mathbb{E}\left\{ \left\| \boldsymbol{z}^{t} \right\|^{2} \right\} \leqslant \frac{8(C_{\alpha})^{2}(G^{2} + \sigma^{2})}{(2C_{\alpha} - 1)^{2}} + \frac{2\epsilon^{2}}{(2C_{\alpha} - 1)^{2}}.$$
 (45)

Proof: Please refer to Appendix E.

Under Assumption 7, Lemmas 1 and 2, and recalling the definition of p^t as given in (40), we have

$$\mathbb{E}\left\{F(\boldsymbol{w}^{t+1}) - F(\boldsymbol{w}^{t})\right\}
\leqslant \mathbb{E}\left\{\left\langle\nabla F(\boldsymbol{w}^{t}), \boldsymbol{w}^{t+1} - \boldsymbol{w}^{t}\right\rangle\right\} + \frac{L}{2}\mathbb{E}\left\{\left\|\boldsymbol{w}^{t+1} - \boldsymbol{w}^{t}\right\|^{2}\right\}
(46a)$$

$$= -\eta^{t}\mathbb{E}\left\{\left\langle\nabla F(\boldsymbol{w}^{t}), \boldsymbol{z}^{t}\right\rangle\right\} + \frac{(\eta^{t})^{2}L}{2}\mathbb{E}\left\{\left\|\boldsymbol{z}^{t}\right\|^{2}\right\}
(46b)$$

$$= \frac{\eta^{t}}{2}\mathbb{E}\left\{\left\|\boldsymbol{z}^{t} - \nabla F(\boldsymbol{w}^{t})\right\|^{2}\right\} - \frac{\eta^{t}}{2}\mathbb{E}\left\{\left\|\nabla F(\boldsymbol{w}^{t})\right\|^{2}\right\}
+ \frac{(\eta^{t})^{2}L - \eta^{t}}{2}\mathbb{E}\left\{\left\|\boldsymbol{z}^{t}\right\|^{2}\right\}
(46c)$$

$$= \frac{\eta^{t}}{2}\mathbb{E}\left\{\left\|\boldsymbol{z}^{t} - \nabla F(\boldsymbol{w}^{t})\right\|^{2}\right\} - \frac{\eta^{t}}{2}\mathbb{E}\left\{\left\|\nabla F(\boldsymbol{w}^{t})\right\|^{2}\right\}
+ \frac{(\eta^{t})^{2}L - \eta^{t}}{2}p^{t}\mathbb{E}\left\{\left\|\boldsymbol{z}^{t}\right\|^{2}\right\}
(46d)$$

$$\leqslant -\frac{\eta^{t}}{2}\mathbb{E}\left\{\left\|\nabla F(\boldsymbol{w}^{t})\right\|^{2}\right\} + \frac{\eta^{t}}{2}\Delta^{t}$$

$$+ \frac{(\eta^{t} + p^{t}(\eta^{t})^{2}L - p^{t}\eta^{t})\epsilon^{2}}{(2C_{\alpha} - 1)^{2}}$$

$$+ \frac{4(C_{\alpha})^{2}(\eta^{t}\sigma^{2} + (p^{t}(\eta^{t})^{2}L - p^{t}\eta^{t})(G^{2} + \sigma^{2}))}{(2C_{\alpha} - 1)^{2}}.$$
(46e)

Summarizing the inequality in (46) for t = 1, 2, ..., T and dividing the summarized inequality with $\sum_{t=1}^{T} \eta^t / 2$ for both

sides, we obtain

$$\sum_{t=1}^{T} \frac{\eta^{t}}{\sum_{t'=1}^{T} \eta^{t}} \mathbb{E}\left\{ \left\| \nabla F(\boldsymbol{w}^{t}) \right\|^{2} \right\}
\leq \frac{2\mathbb{E}\left\{ F(\boldsymbol{w}^{1}) - F(\boldsymbol{w}^{T}) \right\}}{\sum_{t'=1}^{T} \eta^{t}} + \frac{1}{\sum_{t=1}^{T} \eta^{t}} \sum_{t=1}^{T} \eta^{t} \Delta^{t}
+ \sum_{t=1}^{T} \frac{2(\eta^{t} + p^{t}(\eta^{t})^{2}L - p^{t}\eta^{t})\epsilon^{2}}{(2C_{\alpha} - 1)^{2} \sum_{t'=1}^{T} \eta^{t}}
+ \sum_{t=1}^{T} \frac{8(C_{\alpha})^{2}(\eta^{t}\sigma^{2} + (p^{t}(\eta^{t})^{2}L - p^{t}\eta^{t})(G^{2} + \sigma^{2}))}{(2C_{\alpha} - 1)^{2} \sum_{t'=1}^{T} \eta^{t}}.$$
(47)

This completes the proof of Theorem 3.

APPENDIX C PROOF OF THEOREM 4

With Assumptions 7 and the fact that $\nabla F(\boldsymbol{w}^*) = \mathbf{0}$, there is

$$\mathbb{E}\left\{F(\boldsymbol{w}^{t+1}) - F(\boldsymbol{w}^*)\right\}$$

$$\leq \mathbb{E}\left\{\left\langle\nabla F(\boldsymbol{w}^*), \boldsymbol{w}^{t+1} - \boldsymbol{w}^*\right\rangle\right\} + \frac{L}{2}\mathbb{E}\left\{\left\|\boldsymbol{w}^{t+1} - \boldsymbol{w}^*\right\|^2\right\}$$
(48a)
$$= \frac{L}{2}\mathbb{E}\left\{\left\|\boldsymbol{w}^{t+1} - \boldsymbol{w}^*\right\|^2\right\}.$$
(48b)

For the term $\mathbb{E}\left\{\left\|m{w}^{t+1}-m{w}^*\right\|^2\right\}$, with $0<\lambda^t<1$, it leads

$$\mathbb{E}\left\{\left\|\boldsymbol{w}^{t+1} - \boldsymbol{w}^{*}\right\|^{2}\right\} \\
= \mathbb{E}\left\{\left\|\boldsymbol{w}^{t+1} - \boldsymbol{w}^{t} + \eta^{t} \nabla F(\boldsymbol{w}^{t}) + \boldsymbol{w}^{t} - \eta^{t} \nabla F(\boldsymbol{w}^{t}) - \boldsymbol{w}^{*}\right\|^{2}\right\} \tag{49a}$$

$$\leqslant \frac{1}{\lambda^{t}} \mathbb{E}\left\{\left\|\boldsymbol{w}^{t+1} - \boldsymbol{w}^{t} + \eta^{t} \nabla F(\boldsymbol{w}^{t})\right\|^{2}\right\} \tag{49b}$$

$$+ \frac{1}{1 - \lambda^{t}} \mathbb{E}\left\{\left\|\boldsymbol{w}^{t} - \eta^{t} \nabla F(\boldsymbol{w}^{t}) - \boldsymbol{w}^{*}\right\|^{2}\right\} \tag{49b}$$

$$= \frac{(\eta^{t})^{2}}{\lambda^{t}} \mathbb{E}\left\{\left\|\boldsymbol{z}^{t} - \nabla F(\boldsymbol{w}^{t})\right\|^{2}\right\} + \frac{1}{1 - \lambda^{t}} \mathbb{E}\left\{\left\|\boldsymbol{w}^{t} - \boldsymbol{w}^{*}\right\|^{2}\right\}$$

$$- \frac{2\eta^{t}}{1 - \lambda^{t}} \left\langle \boldsymbol{w}^{t} - \boldsymbol{w}^{*}, \nabla F(\boldsymbol{w}^{t}) - \nabla F(\boldsymbol{w}^{*})\right\rangle$$

$$+ \frac{(\eta^{t})^{2}}{1 - \lambda^{t}} \mathbb{E}\left\{\left\|\nabla F(\boldsymbol{w}^{t}) - \nabla F(\boldsymbol{w}^{*})\right\|^{2}\right\}$$

$$\leqslant \frac{(\eta^{t})^{2}}{\lambda^{t}} \mathbb{E}\left\{\left\|\boldsymbol{z}^{t} - \nabla F(\boldsymbol{w}^{t})\right\|^{2}\right\}$$

$$+ \frac{1 - 2\mu\eta^{t} + L^{2}(\eta^{t})^{2}}{1 - \lambda^{t}} \mathbb{E}\left\{\left\|\boldsymbol{w}^{t} - \boldsymbol{w}^{*}\right\|^{2}\right\}, \tag{49d}$$

where

- the inequality (49b) comes from Cauchy-Schwarz inequality $\left(\frac{a^2}{c} + \frac{b^2}{1-c}\right)(c+1-c) \geqslant (a+b)^2, 0 < c < 1;$
- the equality (49c) is established because of $\nabla F(w^*) = 0$;
- the inequality (49d) is bounded by Assumptions 7 and 8.

Applying the inequality in (49) for t=1,2,...,T, and recalling that $\gamma^t=\frac{1-2\mu\eta^t+L^2(\eta^t)^2}{1-\lambda^t}$ and the definition of q^t , we then have

$$\mathbb{E}\left\{\left\|\boldsymbol{w}^{T} - \boldsymbol{w}^{*}\right\|^{2}\right\} \leqslant \prod_{t=1}^{T-1} \gamma^{t} \mathbb{E}\left\{\left\|\boldsymbol{w}^{1} - \boldsymbol{w}^{*}\right\|^{2}\right\} + \sum_{t=1}^{T-1} \frac{(\eta^{t})^{2}}{\lambda^{t}} \prod_{i=t}^{T-1} (\gamma^{i+1})^{q^{i+1}} \mathbb{E}\left\{\left\|\boldsymbol{z}^{t} - \nabla F(\boldsymbol{w}^{t})\right\|^{2}\right\}. (50)$$

With the help of Lemma 1, and combining (48) and (50), there is

$$\mathbb{E}\left\{F(\boldsymbol{w}^{T}) - F(\boldsymbol{w}^{*})\right\}
\leqslant \frac{L}{2}\mathbb{E}\left\{\left\|\boldsymbol{w}^{1} - \boldsymbol{w}^{*}\right\|^{2}\right\} \prod_{t=1}^{T-1} \gamma^{t} + \frac{L}{2} \sum_{t=1}^{T-1} \frac{(\eta^{t})^{2}}{\lambda^{t}} \left[\Delta^{t} + \frac{8\sigma^{2}(C_{\alpha})^{2}}{(2C_{\alpha} - 1)^{2}} + \frac{2\epsilon^{2}}{(2C_{\alpha} - 1)^{2}}\right] \cdot \prod_{i=t}^{T-1} (\gamma^{i+1})^{q^{i+1}}.$$
(51)

This completes the proof of Theorem 4.

APPENDIX D PROOF OF LEMMA 1

The proof of Lemma 1 relies on Lemma 3, i.e.,

Lemma 3: Let $\mathcal{Z} = \{z_1, z_2, ..., z_M\}$ be a set of uploaded vectors by M users. The \mathcal{Z} contains B Byzantine attack vectors, which compose of a subset \mathcal{Z}' . When $C_{\alpha} > 0.5$, there is

$$\mathbb{E}\left\{\left\|\operatorname{geomed}\left(\left\{\boldsymbol{z}_{m}|m\in\mathcal{M}\right\},\epsilon\right)\right\|^{2}\right\}$$

$$\leq \frac{8C_{\alpha}}{(2C_{\alpha}-1)^{2}}\sum_{\boldsymbol{z}_{i}\in\mathcal{Z}\backslash\mathcal{Z}'}\alpha_{i}\mathbb{E}\left\|\boldsymbol{z}_{i}\right\|^{2} + \frac{2\epsilon^{2}}{\left(2C_{\alpha}-1\right)^{2}}.$$
 (52)

Proof: Please refer to Appendix F.

With Lemma 3, there is

$$\mathbb{E}\left\{\left\|\boldsymbol{z}^{t} - \nabla F(\boldsymbol{w}^{t})\right\|^{2}\right\} \leqslant \frac{2\epsilon^{2}}{(2C_{\alpha} - 1)^{2}} + \frac{8C_{\alpha}}{(2C_{\alpha} - 1)^{2}} \sum_{m \in \mathcal{M} \setminus \mathcal{B}} \alpha_{m} \mathbb{E}\left\|\boldsymbol{z}_{m}^{t} - \nabla F(\boldsymbol{w}^{t})\right\|^{2}, \quad (53)$$

since $\mathbf{z}^t - \nabla F(\mathbf{w}^t) = \text{geomed} \left(\{ \mathbf{z}_m^t - \nabla F(\mathbf{w}^t) | m \in \mathcal{M} \}, \epsilon \right).$

For the term $\mathbb{E}\left\{\left\|\boldsymbol{z}_{m}^{t}-\nabla F(\boldsymbol{w}^{t})\right\|^{2}\right\}$, $m\in\mathcal{M}\setminus\mathcal{B}$, we have

$$\mathbb{E}\left\{\left\|\boldsymbol{z}_{m}^{t} - \nabla F(\boldsymbol{w}^{t})\right\|^{2}\right\} \\
= \mathbb{E}\left\{\left\|\frac{1}{K^{t}}\sum_{k=1}^{K^{t}} \nabla F_{m}(\boldsymbol{w}_{m}^{t,k-1}; \boldsymbol{\xi}_{m}^{t,k}) - \nabla F(\boldsymbol{w}^{t})\right\|^{2}\right\} \quad (54a)$$

$$= \frac{1}{(K^{t})^{2}}\mathbb{E}\left\{\left\|\sum_{k=1}^{K^{t}} \left(\nabla F_{m}(\boldsymbol{w}_{m}^{t,k-1}; \boldsymbol{\xi}_{m}^{t,k}) - \nabla F(\boldsymbol{w}^{t})\right)\right\|^{2}\right\} \quad (54b)$$

$$\leq \frac{1}{K^{t}}\sum_{k=1}^{K^{t}}\mathbb{E}\left\{\left\|\nabla F_{m}(\boldsymbol{w}_{m}^{t,k-1}; \boldsymbol{\xi}_{m}^{t,k}) - \nabla F(\boldsymbol{w}^{t})\right\|^{2}\right\} \quad (54c)$$

$$= \frac{1}{K^{t}}\sum_{k=1}^{K^{t}}\mathbb{E}\left\{\left\|\nabla F_{m}(\boldsymbol{w}_{m}^{t,k-1}; \boldsymbol{\xi}_{m}^{t,k}) - \nabla F_{m}(\boldsymbol{w}_{m}^{t,k-1}) + \nabla F_{m}(\boldsymbol{w}_{m}^{t,k-1}) - \nabla F(\boldsymbol{w}^{t})\right\|^{2}\right\} \quad (54d)$$

$$= \frac{1}{K^{t}}\sum_{k=1}^{K^{t}}\mathbb{E}\left\{\left\|\nabla F_{m}(\boldsymbol{w}_{m}^{t,k-1}; \boldsymbol{\xi}_{m}^{t,k}) - \nabla F_{m}(\boldsymbol{w}_{m}^{t,k-1})\right\|^{2} + \left\|\nabla F_{m}(\boldsymbol{w}_{m}^{t,k-1}) - \nabla F(\boldsymbol{w}^{t})\right\|^{2} + 2\left\langle\nabla F_{m}(\boldsymbol{w}_{m}^{t,k-1}; \boldsymbol{\xi}_{m}^{t,k}) - \nabla F_{m}(\boldsymbol{w}_{m}^{t,k-1}), \\ \nabla F_{m}(\boldsymbol{w}_{m}^{t,k-1}) - \nabla F(\boldsymbol{w}^{t})\right\rangle^{2}, \quad (54e)$$

where the inequality (54c) holds because of the Cauchy-Schwarz inequality $(a_1+a_2+a_3+\cdots+a_n)^2\leqslant n(a_1^2+a_2^2+a_3^2+\cdots+a_n^2)$. With Assumptions 9 and 10, there are $\mathbb{E}\left\{\nabla F_m(\boldsymbol{w}_m^{t,k-1};\boldsymbol{\xi}_m^{t,k})-\nabla F_m(\boldsymbol{w}_m^{t,k-1})\right\}=0$ and $\mathbb{E}\left\{\left\|\nabla F_m(\boldsymbol{w}_m^{t,k-1};\boldsymbol{\xi}_m^{t,k})-\nabla F_m(\boldsymbol{w}_m^{t,k-1})\right\|^2\right\}\leqslant\sigma^2$, then (54) leads to

$$\mathbb{E}\left\{\left\|\boldsymbol{z}_{m}^{t} - \nabla F(\boldsymbol{w}^{t})\right\|^{2}\right\}
\leqslant \frac{1}{K^{t}} \sum_{k=1}^{K^{t}} \mathbb{E}\left\{\left\|\nabla F_{m}(\boldsymbol{w}_{m}^{t,k-1}) - \nabla F(\boldsymbol{w}^{t})\right\|^{2}\right\} + \sigma^{2} \quad (55a)$$

$$= \frac{1}{K^{t}} \sum_{k=1}^{K^{t}} \mathbb{E}\left\{\left\|\nabla F_{m}(\boldsymbol{w}_{m}^{t,k-1}) - \nabla F(\boldsymbol{w}_{m}^{t,k-1}) + \nabla F(\boldsymbol{w}_{m}^{t,k-1}) - \nabla F(\boldsymbol{w}^{t})\right\|^{2}\right\} + \sigma^{2} \quad (55b)$$

$$\leqslant \frac{2}{K^{t}} \sum_{k=1}^{K^{t}} \mathbb{E}\left\{\left\|\nabla F(\boldsymbol{w}_{m}^{t,k-1}) - \nabla F(\boldsymbol{w}^{t})\right\|^{2}\right\}$$

$$+ \frac{2}{K^{t}} \sum_{k=1}^{K^{t}} \mathbb{E}\left\{\left\|\nabla F_{m}(\boldsymbol{w}_{m}^{t,k}) - \nabla F(\boldsymbol{w}_{m}^{t,k})\right\|^{2}\right\} + \sigma^{2},$$

$$(55c)$$

where the inequality (55c) can be derived from $(a + b)^2 \le 2a^2 + 2b^2$.

To further upper bound the right-hand side of (55), since $(\theta_m^{t,k})^2 = \|\nabla F_m(\boldsymbol{w}_m^{t,k}) - \nabla F(\boldsymbol{w}_m^{t,k})\|^2 \leqslant \theta^2$, we only need

to inspect the bound of $\sum_{k=0}^{K^t} \mathbb{E}\left\{\left\|\nabla F(\boldsymbol{w}_m^{t,k-1}) - \nabla F(\boldsymbol{w}^t)\right\|^2\right\}$, which is given as follows

$$\sum_{k=1}^{K^{t}} \mathbb{E} \left\{ \left\| \nabla F(\boldsymbol{w}_{m}^{t,k-1}) - \nabla F(\boldsymbol{w}^{t}) \right\|^{2} \right\}
\leqslant L^{2} \sum_{k=1}^{K^{t}} \mathbb{E} \left\{ \left\| \boldsymbol{w}_{m}^{t,k-1} - \boldsymbol{w}^{t} \right\|^{2} \right\}
= L^{2} \sum_{k=2}^{K^{t}} \mathbb{E} \left\{ \left\| \sum_{i=1}^{k-1} \eta_{m}^{t,i} \cdot \nabla F_{m}(\boldsymbol{w}_{m}^{t,i-1}; \boldsymbol{\xi}_{m}^{t,i}) \right\|^{2} \right\}
\leqslant L^{2} \sum_{k=2}^{K^{t}} \left(\sum_{i=1}^{k-1} (\eta_{m}^{t,i})^{2} \cdot \sum_{i=1}^{k-1} \mathbb{E} \left\{ \left\| \nabla F_{m}(\boldsymbol{w}_{m}^{t,i-1}; \boldsymbol{\xi}_{m}^{t,i}) \right\|^{2} \right\} \right)$$
(56b)

$$\leqslant L^2 \sum_{k=2}^{K^t} \left(\sum_{i=1}^{k-1} (\eta_m^{t,i})^2 \cdot (k-1)(G^2 + \sigma^2) \right) \tag{56d}$$

$$=L^{2}(G^{2}+\sigma^{2})\sum_{k=2}^{K^{t}}(k-1)\sum_{i=1}^{k-1}(\eta_{m}^{t,i})^{2},$$
(56e)

where

- the inequality (56a) holds according to Assumption 7;
- the inequality (56c) comes from Cauchy-Schwarz inequality $(a_1b_1 + a_2b_2 + a_3b_3 + \dots + a_nb_n)^2 \le (a_1^2 + a_2^2 + a_3^2 + \dots + a_n^2)(b_1^2 + b_2^2 + b_3^2 + \dots + b_n^2);$
- the inequality (56d) can be derived from Assumptions 9,

Combining (42), (53), (55) and (56), we obtain the following inequality

$$\mathbb{E}\left\{\left\|\boldsymbol{z}^{t} - \nabla F(\boldsymbol{w}^{t})\right\|^{2}\right\} \leqslant \Delta^{t} + \frac{8\sigma^{2}(C_{\alpha})^{2}}{(2C_{\alpha} - 1)^{2}} + \frac{2\epsilon^{2}}{(2C_{\alpha} - 1)^{2}}. \qquad \sum_{i=1}^{M} \alpha_{i} \left\|\boldsymbol{z}^{*} - \boldsymbol{z}_{i}\right\| = \inf_{\boldsymbol{y}} \sum_{i=1}^{M} \alpha_{i} \left\|\boldsymbol{y} - \boldsymbol{z}_{i}\right\| \leqslant \sum_{i=1}^{M} \alpha_{i} \left\|\boldsymbol{z}_{i}\right\|.$$

This completes the proof of Lemma 1.

APPENDIX E PROOF OF LEMMA 2

With Lemma 3, there is

$$\mathbb{E}\left\{\left\|\boldsymbol{z}^{t}\right\|^{2}\right\} \leqslant \frac{8C_{\alpha}}{(2C_{\alpha}-1)^{2}} \sum_{m \in \mathcal{M} \setminus \mathcal{B}} \alpha_{m} \mathbb{E}\left\|\boldsymbol{z}_{m}^{t}\right\|^{2} + \frac{2\epsilon^{2}}{(2C_{\alpha}-1)^{2}}.$$
(58)

For the term $\mathbb{E}\left\{\left\|\boldsymbol{z}_{m}^{t}\right\|^{2}\right\}$, $m\in\mathcal{M}\setminus\mathcal{B}$, according to Assumptions 9, 10 and 12, we have

$$\mathbb{E}\left\{\left\|\boldsymbol{z}_{m}^{t}\right\|^{2}\right\} = \mathbb{E}\left\{\left\|\frac{1}{K^{t}}\sum_{k=1}^{K^{t}}\nabla F_{m}(\boldsymbol{w}_{m}^{t,k-1};\boldsymbol{\xi}_{m}^{t,k})\right\|^{2}\right\}$$
(59a)
$$\leq \frac{1}{K^{t}}\sum_{k=1}^{K^{t}}\mathbb{E}\left\{\left\|\nabla F_{m}(\boldsymbol{w}_{m}^{t,k-1};\boldsymbol{\xi}_{m}^{t,k})\right\|^{2}\right\}$$
(59b)
$$\leq G^{2} + \sigma^{2},$$
(59c)

where the inequality (59b) comes from Cauchy-Schwarz inequality $(a_1 + a_2 + a_3 + \dots + a_n)^2 \le n(a_1^2 + a_2^2 + a_3^2 + \dots + a_n^2)$. Hence we can get the following inequality

$$\mathbb{E}\left\{ \left\| \boldsymbol{z}^{t} \right\|^{2} \right\} \leqslant \frac{8(C_{\alpha})^{2}(G^{2} + \sigma^{2})}{(2C_{\alpha} - 1)^{2}} + \frac{2\epsilon^{2}}{(2C_{\alpha} - 1)^{2}}.$$
 (60)

Since $\mathbb{E}\left\{\left\|\boldsymbol{z}^t\right\|^2\right\} \geqslant 0$, then there is

$$0 \leqslant \mathbb{E}\left\{ \left\| \boldsymbol{z}^{t} \right\|^{2} \right\} \leqslant \frac{8(C_{\alpha})^{2}(G^{2} + \sigma^{2})}{(2C_{\alpha} - 1)^{2}} + \frac{2\epsilon^{2}}{(2C_{\alpha} - 1)^{2}}. \tag{61}$$

This completes the proof of Lemma 2.

APPENDIX F PROOF OF LEMMA 3

For the ease of presentation, we denote $egin{aligned} oldsymbol{z}^* &= \operatorname{geomed}\left(\{oldsymbol{z}_m | m \in \mathcal{M}\}\right) \text{ and } \ oldsymbol{z}^*_{\epsilon} &= \operatorname{geomed}\left(\{oldsymbol{z}_m | m \in \mathcal{M}\}, \epsilon\right), \text{ then there is } \end{aligned}$

$$\sum_{i=1}^{M} \frac{S_i}{\sum_{j=1}^{M} S_j} \| \boldsymbol{z}_{\epsilon}^* - \boldsymbol{z}_i \| \leq \sum_{i=1}^{M} \frac{S_i}{\sum_{j=1}^{M} S_j} \| \boldsymbol{z}^* - \boldsymbol{z}_i \| + \epsilon,$$
(62)

which implies

$$\sum_{i=1}^{M} \alpha_i \| \boldsymbol{z}_{\epsilon}^* - \boldsymbol{z}_i \| \leqslant \sum_{i=1}^{M} \alpha_i \| \boldsymbol{z}^* - \boldsymbol{z}_i \| + \epsilon, \quad (63)$$

by recalling the definition of α_i as given in (39). By the definition of geometric median, there is

$$\sum_{i=1}^{M} \alpha_i \|\boldsymbol{z}^* - \boldsymbol{z}_i\| = \inf_{\boldsymbol{y}} \sum_{i=1}^{M} \alpha_i \|\boldsymbol{y} - \boldsymbol{z}_i\| \leqslant \sum_{i=1}^{M} \alpha_i \|\boldsymbol{z}_i\|.$$
(64)

According to the triangle inequality, we have

$$\sum_{\boldsymbol{z}_{i} \in \mathcal{Z}'} \alpha_{i} \|\boldsymbol{z}_{\epsilon}^{*} - \boldsymbol{z}_{i}\| \geqslant \sum_{\boldsymbol{z}_{i} \in \mathcal{Z}'} \alpha_{i} (\|\boldsymbol{z}_{i}\| - \|\boldsymbol{z}_{\epsilon}^{*}\|), \quad (65)$$

$$\sum_{\boldsymbol{z}_{i} \in \mathcal{Z} \setminus \mathcal{Z}'} \alpha_{i} \|\boldsymbol{z}_{\epsilon}^{*} - \boldsymbol{z}_{i}\| \geqslant \sum_{\boldsymbol{z}_{i} \in \mathcal{Z} \setminus \mathcal{Z}'} \alpha_{i} (\|\boldsymbol{z}_{\epsilon}^{*}\| - \|\boldsymbol{z}_{i}\|). \quad (66)$$

By adding (65) and (66) together, we obtain

$$\sum_{\boldsymbol{z}_{i} \in \mathcal{Z}} \alpha_{i} \|\boldsymbol{z}_{\epsilon}^{*} - \boldsymbol{z}_{i}\| \geqslant \sum_{\boldsymbol{z}_{i} \in \mathcal{Z}} \alpha_{i} \|\boldsymbol{z}_{i}\| + \left(1 - \sum_{\boldsymbol{z}_{i} \in \mathcal{Z}'} 2\alpha_{i}\right) \|\boldsymbol{z}_{\epsilon}^{*}\| - 2 \sum_{\boldsymbol{z}_{i} \in \mathcal{Z} \setminus \mathcal{Z}'} \alpha_{i} \|\boldsymbol{z}_{i}\|.$$

$$(67)$$

Combining (63), (64), and (67), and with the fact that $\sum_{\boldsymbol{z}_i \in \mathcal{Z}'} \alpha_i = 1 - C_\alpha < 1/2, \text{ we have the following inequality}$

$$\|\boldsymbol{z}_{\epsilon}^*\| \leqslant \frac{2\sum_{\boldsymbol{z}_i \in \mathcal{Z} \setminus \mathcal{Z}'} \alpha_i \|\boldsymbol{z}_i\| + \epsilon}{1 - 2\sum_{\boldsymbol{z}_i \in \mathcal{Z}'} \alpha_i}.$$
 (68)

Squaring both sides of (68) and based on the Cauchy-Schwarz inequality, we further have

$$\|\boldsymbol{z}_{\epsilon}^{*}\|^{2} \leq \left(\frac{2\sum_{\boldsymbol{z}_{i}\in\mathcal{Z}\backslash\mathcal{Z}'}\alpha_{i}\|\boldsymbol{z}_{i}\|+\epsilon}{1-2\sum_{\boldsymbol{z}_{i}\in\mathcal{Z}'}\alpha_{i}}\right)^{2}$$

$$\leq \frac{8\left(\sum_{\boldsymbol{z}_{i}\in\mathcal{Z}\backslash\mathcal{Z}'}\alpha_{i}\|\boldsymbol{z}_{i}\|\right)^{2}+2\epsilon^{2}}{\left(1-2\sum_{\boldsymbol{z}_{i}\in\mathcal{Z}'}\alpha_{i}\right)^{2}}$$

$$= \frac{8\left(\sum_{\boldsymbol{z}_{i}\in\mathcal{Z}\backslash\mathcal{Z}'}\alpha_{i}\right)^{2}}{\left(1-2\sum_{\boldsymbol{z}_{i}\in\mathcal{Z}'}\alpha_{i}\right)^{2}} \left(\sum_{\boldsymbol{z}_{i}\in\mathcal{Z}\backslash\mathcal{Z}'}\frac{\alpha_{i}}{\sum_{\boldsymbol{z}_{j}\in\mathcal{Z}\backslash\mathcal{Z}'}\alpha_{j}}\|\boldsymbol{z}_{i}\|\right)^{2}$$

$$+ \frac{2\epsilon^{2}}{\left(1-2\sum_{\boldsymbol{z}_{i}\in\mathcal{Z}'}\alpha_{i}\right)^{2}}$$

$$\leq \frac{8\left(\sum_{\boldsymbol{z}_{i}\in\mathcal{Z}\backslash\mathcal{Z}'}\alpha_{i}\right)\sum_{\boldsymbol{z}_{i}\in\mathcal{Z}\backslash\mathcal{Z}'}\alpha_{i}\|\boldsymbol{z}_{i}\|^{2}+2\epsilon^{2}}{\left(1-2\sum_{\boldsymbol{z}_{i}\in\mathcal{Z}\backslash\mathcal{Z}'}\alpha_{i}\right)\sum_{\boldsymbol{z}_{i}\in\mathcal{Z}\backslash\mathcal{Z}'}\alpha_{i}\|\boldsymbol{z}_{i}\|^{2}+2\epsilon^{2}},$$

$$\leq \frac{8\left(\sum_{\boldsymbol{z}_{i}\in\mathcal{Z}\backslash\mathcal{Z}'}\alpha_{i}\right)\sum_{\boldsymbol{z}_{i}\in\mathcal{Z}\backslash\mathcal{Z}'}\alpha_{i}\|\boldsymbol{z}_{i}\|^{2}+2\epsilon^{2}}{\left(1-2\sum_{\boldsymbol{z}_{i}\in\mathcal{Z}'}\alpha_{i}\right)^{2}},$$

$$\leq \frac{8\left(\sum_{\boldsymbol{z}_{i}\in\mathcal{Z}\backslash\mathcal{Z}'}\alpha_{i}\right)\sum_{\boldsymbol{z}_{i}\in\mathcal{Z}\backslash\mathcal{Z}'}\alpha_{i}\|\boldsymbol{z}_{i}\|^{2}+2\epsilon^{2}}{\left(1-2\sum_{\boldsymbol{z}_{i}\in\mathcal{Z}'}\alpha_{i}\right)^{2}},$$

$$\leq \frac{8\left(\sum_{\boldsymbol{z}_{i}\in\mathcal{Z}\backslash\mathcal{Z}'}\alpha_{i}\right)\sum_{\boldsymbol{z}_{i}\in\mathcal{Z}\backslash\mathcal{Z}'}\alpha_{i}\|\boldsymbol{z}_{i}\|^{2}+2\epsilon^{2}}{\left(1-2\sum_{\boldsymbol{z}_{i}\in\mathcal{Z}'}\alpha_{i}\right)^{2}},$$

$$\leq \frac{8\left(\sum_{\boldsymbol{z}_{i}\in\mathcal{Z}\backslash\mathcal{Z}'}\alpha_{i}\right)\sum_{\boldsymbol{z}_{i}\in\mathcal{Z}\backslash\mathcal{Z}'}\alpha_{i}\|\boldsymbol{z}_{i}\|^{2}+2\epsilon^{2}}{\left(1-2\sum_{\boldsymbol{z}_{i}\in\mathcal{Z}'}\alpha_{i}\right)^{2}},$$

$$\leq \frac{8\left(\sum_{\boldsymbol{z}_{i}\in\mathcal{Z}\backslash\mathcal{Z}'}\alpha_{i}\right)\sum_{\boldsymbol{z}_{i}\in\mathcal{Z}\backslash\mathcal{Z}'}\alpha_{i}\|\boldsymbol{z}_{i}\|^{2}+2\epsilon^{2}}{\left(1-2\sum_{\boldsymbol{z}_{i}\in\mathcal{Z}'}\alpha_{i}\right)^{2}},$$

$$\leq \frac{8\left(\sum_{\boldsymbol{z}_{i}\in\mathcal{Z}\backslash\mathcal{Z}'}\alpha_{i}\right)\sum_{\boldsymbol{z}_{i}\in\mathcal{Z}\backslash\mathcal{Z}'}\alpha_{i}\|\boldsymbol{z}_{i}\|^{2}}{\left(1-2\sum_{\boldsymbol{z}_{i}\in\mathcal{Z}'}\alpha_{i}\right)^{2}},$$

where

- the inequality (69b) comes from $(a+b)^2 \le 2a^2 + 2b^2$;
- the inequality (69d) holds because of Jensen's inequality $f\left(\sum_{i=1}^n \nu_i x_i\right) \leqslant \sum_{i=1}^n \nu_i f(x_i) \text{ with } \sum_{i=1}^n \nu_i = 1, \, \nu_i \geq 0 \text{ for } i=1,2,...,n, \text{ and } f(x)=x^2 \text{ being a convex function.}$

Recalling of the definition of C_{α} in (39), we then have

$$\|\boldsymbol{z}_{\epsilon}^{*}\|^{2} \leq \frac{8C_{\alpha}}{(2C_{\alpha}-1)^{2}} \sum_{\boldsymbol{z}_{i} \in \mathcal{Z} \setminus \mathcal{Z}'} \alpha_{i} \|\boldsymbol{z}_{i}\|^{2} + \frac{2\epsilon^{2}}{(2C_{\alpha}-1)^{2}}.$$
 (70)

Taking the expectation of the both sides of (70) can lead to the statement of Lemma 3.